

This is an Open Access document downloaded from ORCA, Cardiff University's institutional repository:<https://orca.cardiff.ac.uk/id/eprint/124939/>

This is the author's version of a work that was submitted to / accepted for publication.

Citation for final published version:

Wang, Dengjia, Liu, Hui, Liu, Yanfeng, Xu, Tao, Wang, Yingying, Du, Hu , Wang, Xiaowen and Liu, Jiaping 2019. Frost and high-temperature resistance performance of a novel dual-phase change material flat plate solar collector. *Solar Energy Materials and Solar Cells* 201 , 110086. 10.1016/j.solmat.2019.110086

Publishers page: <https://doi.org/10.1016/j.solmat.2019.110086>

Please note:

Changes made as a result of publishing processes such as copy-editing, formatting and page numbers may not be reflected in this version. For the definitive version of this publication, please refer to the published source. You are advised to consult the publisher's version if you wish to cite this paper.

This version is being made available in accordance with publisher policies. See <http://orca.cf.ac.uk/policies.html> for usage policies. Copyright and moral rights for publications made available in ORCA are retained by the copyright holders.





1 **Abstract:** In order to overcome the freezing and overheating problems of solar collectors, a novel  
2 dual-phase change material (PCM) flat plate collector was proposed in this research. There were  
3 two layers of PCMs in the solar collector, one layer material with a phase change temperature of  
4 70°C and another with a phase change temperature of 15°C, respectively. They were placed in the  
5 space under the absorber plate in the dual-PCM collector. Frost and High-temperature resistance  
6 performance of the novel dual-phase change material solar collector was tested systematically in a  
7 laboratory. The experimental results showed that the time taken for the temperature of the  
8 absorber plate to increase from 60°C to 78°C could be prolonged by 1.6 h under high temperature  
9 conditions. Furthermore, the low-melting point PCM can substantially slow the temperature  
10 decrease of the collector by solidifying and releasing heat under the low-temperature conditions.  
11 And the time taken for the temperature of the absorber plate to decrease from 19°C to 10°C could  
12 be prolonged by 6.4 h and 3.1 h when low-melting PCM placed below high-melting PCM and the  
13 high-melting PCM placed below low-melting PCM. Thus it can be seen that the dual-PCM  
14 collector can be used to overcome the phenomenon of overheating and freezing. In addition,  
15 compared with an ordinary flat plate collector, the efficiency of the dual-PCM collector was  
16 increased by 24.1% and 19.6% when placing low-melting PCM below high-melting PCM and in  
17 the opposite condition respectively.

18 **Keywords:** Flat plate solar collector; Frost and High-temperature resistance; Phase change  
19 material; Efficiency; Experimental.

## 20 **1. Introduction**

21 Due to the green, renewable and non-emission characteristics of solar energy, solar thermal  
22 utilization systems are widely used [1]. Solar collector is a core component in various solar

1 thermal utilization systems. Its main function is to collect solar radiation energy and transforms  
2  
3 heat energy to thermal users by a solid, liquid, or gas medium. In general, solar collectors are  
4  
5  
6 mainly divided into the following categories: flat plate collectors, heat pipe collectors, vacuum  
7  
8  
9 tube collectors and concentrator collectors. Among these types, flat plate collectors have been  
10  
11  
12 extensively used worldwide due to their simple structure, reliable operation, and low cost and  
13  
14 favorable solar building integration performance [2]. However, there are also two main drawbacks  
15  
16  
17 for flat plate solar collectors of liquid type: the collector would be overheated in the case of  
18  
19  
20 intense solar radiation or with less heat using, and freezing cracks in a low-temperature  
21  
22  
23 environment [3-4]. The flat plate solar collector will receive a substantial amount of energy during  
24  
25  
26 the sunny days, which can easily lead to pipe fouling and system overheating, especially in the  
27  
28  
29 case of heat accumulation. These phenomena can cause pipes to burst and systems to shut down in  
30  
31  
32 severe cases. In low-temperature nighttime environments, water—a common circulating fluid used  
33  
34  
35 in collectors—can easily freeze and damage the collector, which will affect the operation of the  
36  
37  
38 whole system. Therefore, freezing and overheating prevention is essential to extending the service  
39  
40  
41 life of a collector and ensuring the stable and reliable operation of a solar collector system.

42       Currently, overheating problems are mainly handled by the following approaches: application  
43  
44  
45 of heat dumps or heat wasters, venting to remove excess heat, and application of the thermotropic  
46  
47  
48 layers on the absorber or the glazing. [Crofoot and Harrison \[5\]](#) designed a heat waster for the solar  
49  
50  
51 collector array that consists of a control and valving system to exhaust excess heat to the  
52  
53  
54 atmosphere. However, this heat waster is expensive. [H. Kessentini et al. \[6\]](#) proposed a low-cost  
55  
56  
57 anti-overheating collector in which a thermally actuated door installed on the flow channel of the  
58  
59  
60 collector is used to ventilate and prevent the collector from overheating in stagnation conditions

1 and this system can be used to supply the heat from 80 to 120°C. The passive air cooling of flat  
2  
3  
4 plate collectors is studied to solve overheating problems in stagnation conditions, and the results  
5  
6  
7 show that the stagnation temperature 170°C can be decreased to the normal temperature range  
8  
9 [7-8]. Thermotropic material is a unique material of which the transmission properties change with  
10  
11  
12 respect to the temperature, and some researchers [9-11] have studied the application of  
13  
14  
15 thermotropic layers on the glass over and absorber plate of flat plate collectors to provide passive  
16  
17  
18 overheat protection. The methods described above either eliminate the excess heat obtained by the  
19  
20  
21 collectors or reduce the solar energy collected, which would lead to a lot of waste of energy.

22  
23 Freezing problems of the collectors are mainly handled by using the following approaches:  
24  
25  
26 operation adjustment of the system, special design of the flow channel, and reduction of heat loss  
27  
28  
29 in the collector. D. R. Koenigshofer [12] summarized the methods of freeze protection for solar  
30  
31  
32 collectors, including the emptying method, reverse circulation method, and adding antifreeze  
33  
34  
35 liquid. Y. Wei et al. [13] designed a special diamond flow channel which was made of ferritic  
36  
37  
38 stainless steel material to accommodate the expanded volume of water frozen. X. Jiang et al. [14]  
39  
40  
41 used rubber for the upper and lower headers and circulation pipes of solar water heaters and used  
42  
43  
44 high-efficiency copper-aluminum composite strips for the discharge pipes to realize a freezing  
45  
46  
47 sequence of the pipes from the center to the ends according to the theory of sequential freezing,  
48  
49  
50 and the solar water heater can operate normally without other auxiliary equipment. Some  
51  
52  
53 researchers investigated the double glass-cover and the transparent insulation material (TIM) to  
54  
55  
56 lower the heat loss of collectors used in extremely cold areas. A. Ozsoy et al. [15] conducted an  
57  
58  
59 experimental study to a double-glazed flat plate collector and found that the efficiency can be  
60  
61  
62 increased by 24% when the temperature a difference between the water and the environment is  
63  
64  
65

1 40°C. Reddy and Kaushika [16] studied the effect of different configuration of TIM on the heat  
2  
3 loss reduction of the collector. F. Zhou et al. [17, 27] conducted a numerical investigation to the  
4  
5 antifreeze performance of the collector with TIM transparent honeycomb, and the results indicated  
6  
7 that the frozen time could be delayed by 2.5 h. However, these methods would lead to a high cost,  
8  
9 complicate the structure, or reduce the thermal performance of the collector.  
10  
11  
12

13  
14 A phase change material (PCM) can change its physical state by melting and solidifying  
15  
16 within a particular temperature range. And in the process of melting or solidification, the  
17  
18 temperature of a PCM remains approximately constant, which forms a constant temperature  
19  
20 interval for a period of time, and the latent heat absorbed or released is quite large. Therefore, a  
21  
22 PCM can be combined with a flat plate collector to change the heat transfer process of collector  
23  
24 and optimize the corresponding frost resistance and high-temperature resistance.  
25  
26  
27  
28  
29  
30

31 Over the past two decades, a large number of researches have investigated PCM solar  
32  
33 collectors. W. Su et al. [18] added a layer of 5 cm thick inorganic PCM between the absorber and  
34  
35 the insulation of the collector to increase the collector efficiency by 36%. A.E. Kabeel et al. [19]  
36  
37 conducted a study on a PCM (paraffin) air collector with different absorber plates (flat plate and  
38  
39 v-corrugated plate) by experiments, and found that v-corrugated solar collector had a better  
40  
41 thermal performance than the traditional collector with or without PCM, and the v-corrugated  
42  
43 collector with PCM had a 12% higher daily efficiency than that without PCM. Z. Chen et al. [20]  
44  
45 designed a paraffin solar collector wherein the solar energy received by the collector was stored in  
46  
47 paraffin in the form of heat in the day, and the heat is transferred to the working medium by  
48  
49 capillary tubes located inside the paraffin during the nighttime. J. Zhao et al. [21] proposed a PCM  
50  
51 flat plate collector; the solidifying point of their PCM was 277.15~281.15 K, and their simulation  
52  
53  
54  
55  
56  
57  
58  
59  
60  
61  
62  
63  
64  
65

1 results indicated that at the lowest temperature in winter, the minimum temperature of the water  
2  
3 was higher than 275.15 K, which can achieve an antifreeze effect. [A. J. N. Khalifa et al. \[22\]](#)  
4  
5 integrated a heat storage container with solar collector. The back of collector was connected with a  
6  
7 container containing the paraffin as a heat storage medium. The study found that the water of the  
8  
9 pipe can be continuously heated after sunset because of the melting exotherm of the PCM.  
10  
11 [Mettawee and Assassa \[23-24\]](#) experimentally investigated a compact PCM collector and analyzed  
12  
13 the heat transfer characteristics in the melting and solidification process, and their results showed  
14  
15 that the useful heat can be increased by increasing flow rate and adding the aluminum powder to  
16  
17 the PCM. [Y. Varol et al \[25\]](#) experimentally studied a PCM collector using  $\text{NaCO}_3 \cdot \text{H}_2\text{O}$  as the  
18  
19 PCM and found that the useful energy and efficiency of the collector can be enhanced by adding  
20  
21 of PCM and the efficiency increased even solar radiation was reduced. [P. Charvát et al. \[28\]](#)  
22  
23 compared sheet metal collector with the collector composed of nine aluminium plates containing a  
24  
25 paraffin-based PCM (Rubitherm RT 42). Both computer simulations and experimental data show  
26  
27 that latent heat thermal energy storage can effectively lower the fluctuations of outlet air  
28  
29 temperature as the solar radiation intensity changes rapidly, e.g. on cloudy days, but the energy  
30  
31 efficiency of the PCM collector was lower than that of the sheet metal collector. The above studies  
32  
33 mainly used PCMs of a specific melting point to store heat in the daytime and release heat in the  
34  
35 nighttime, which integrates heat collection with heat storage to enhance the thermal performance  
36  
37 of the collector after sunset. However, studies that solve frost cracking or overheating problems of  
38  
39 flat plate collectors using PCM have rarely been reported in the literature.  
40  
41  
42  
43  
44  
45  
46  
47  
48  
49  
50  
51  
52  
53  
54  
55  
56  
57  
58  
59  
60  
61  
62  
63  
64  
65

21 The freezing and overheating problems of the flat plate collector have a severe impact on the  
57  
58 normal working of the collector and the stability of the solar water heating system. However, for  
59  
60  
61  
62  
63  
64  
65

1 the traditional solution, there are problems such as complicated structure, waste of energy and so  
2 on. In addition, it is difficult to apply the traditional method in the case which there are both  
3 cracking and overheating problems during long-term operation of the collector. PCM can absorb  
4 heat when melting and release heat when solidifying. Therefore, applying a layer of high-melting  
5 PCM and a layer of low-melting PCM simultaneously to the collector can alleviate the frost  
6 cracking and overheating problems of the flat plate collector, meanwhile, it avoids the waste of  
7 excess energy and does not increase the complexity of the structure of the collector.

8 To solve the problems of plate collectors (freezing cracks under low-temperature  
9 environments and overheating under strong radiation environments), this paper proposes a  
10 dual-PCM flat plate collector. The collector contains two layers of PCMs with different melting  
11 points of 70°C and 15°C which placed under the absorber plate to relieve the freezing and  
12 overheating problems of the collector. The experiments were performed to investigate the heat  
13 transfer process and the efficiency of the PCM collector. The delay effect of the PCMs on the  
14 highest and lowest temperature point of the collector was researched by comparing the  
15 temperature and heat fluxes of the conventional and PCM collectors, and the thermal performance  
16 improvement of the PCMs on the collector is studied through the efficiency calculation.

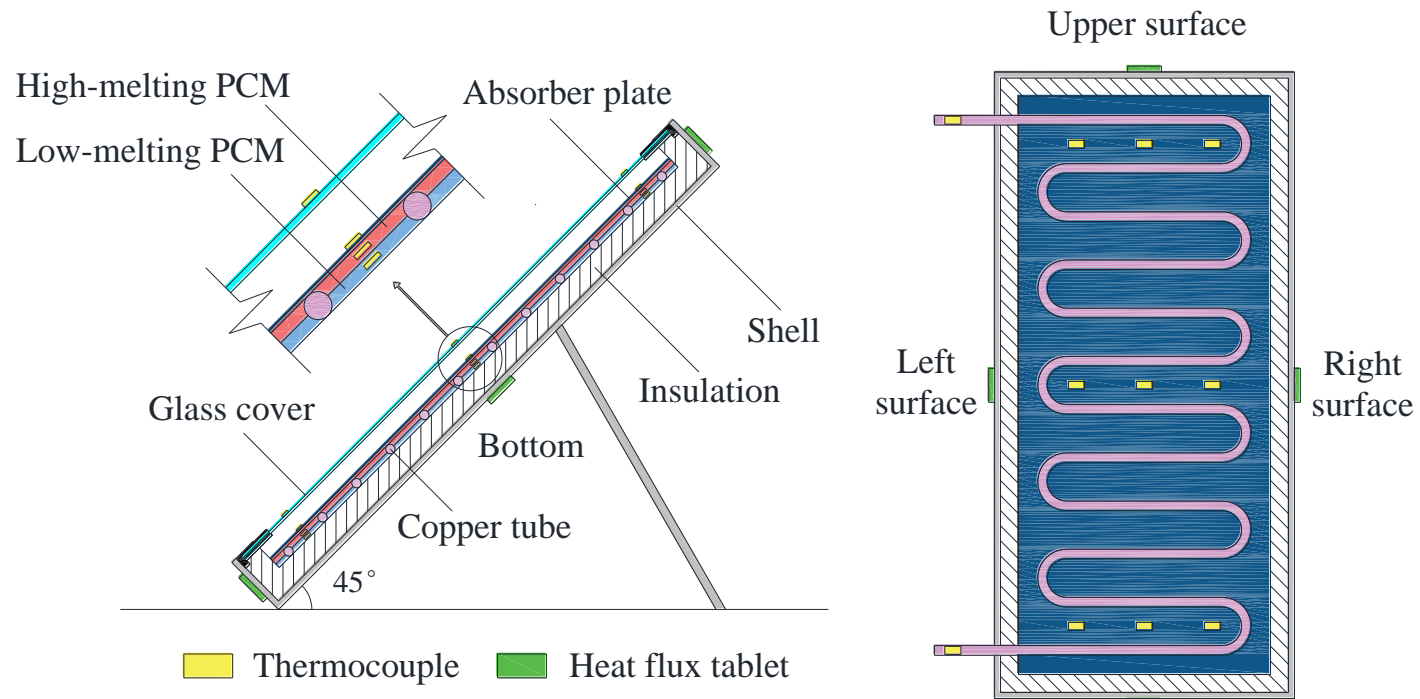
## 17 18 **2. Methodology**

### 19 **2.1 PCM collector design**

20 The structure of the proposed PCM collector is shown in Fig. 1, and the image of the PCM  
21 collector is shown in Fig. 2. An s-shaped pipe is located below the absorber plate, and two kinds  
22 of PCMs (a “high-melting PCM” with a phase change temperature of 70°C and a “low-melting

1 PCM” with a phase change temperature of 15°C) wrapped with aluminum foil are placed in the  
2  
3 space area under the absorber plate, respectively. In this research, three types of collectors were  
4  
5 experimentally compared, which were the collector with low-melting PCM under high-melting  
6  
7 PCM, the collector with high-melting PCM under low-melting PCM, and the collector without  
8  
9 PCM. Under intense radiation, high-temperature environment, when the water temperature causes  
10  
11 the high-melting PCM temperature to exceed 70°C, the PCM will melt and absorb heat to protect  
12  
13 the working fluid from overheating. In a low-temperature condition, when the temperature of the  
14  
15 low-melting PCM is less than 15°C, the PCM will solidify and release heat to protect the working  
16  
17 fluid from freezing. The experiment chose a kind of high thermal conductivity PCM that was  
18  
19 encapsulated in spherical particles and maintained a solid form after melting, and the PCM was  
20  
21 made of 20% high-purity graphite and 80% natural grease. A picture and the physical parameters  
22  
23 of the spherical particle PCMs are shown in Fig. 3 and Table 1, respectively. The specific design  
24  
25 parameters of the PCM collector are listed in Table 2.  
26  
27  
28  
29  
30  
31  
32  
33  
34  
35  
36  
37  
38  
39  
40  
41  
42  
43  
44  
45  
46  
47  
48  
49  
50  
51  
52  
53  
54  
55  
56  
57  
58  
59  
60  
61  
62  
63  
64  
65

1  
2  
3  
4  
5  
6  
7  
8  
9  
10  
11  
12  
13  
14  
15  
16  
17  
18  
19  
20  
21  
22  
23  
24  
25  
26  
27  
28  
29  
30  
31  
32  
33  
34  
35  
36  
37  
38  
39  
40  
41  
42  
43  
44  
45  
46  
47  
48  
49



1

2

Fig. 1 Structure of the PCM collector and sensor locations

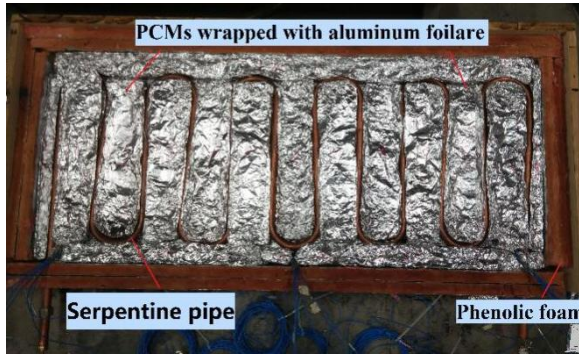


Fig. 2 Location of the PCMs in the collector

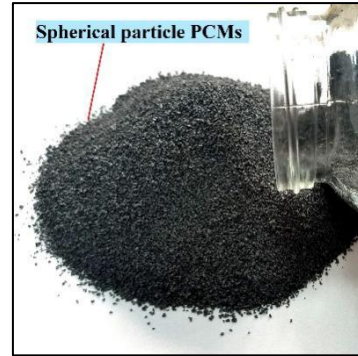


Fig. 3 Spherical particle PCMs

Table 1 Physical parameters of the two kinds of PCMs

Phase transition temperature (°C)	Latent heat (J/g)	Thermal Conductivity (W/(m·K))	Density (g/mL)	Specific heat capacity (J/(g·K))
15	190	3-5	0.87	2
70	210	3-5	0.97	2

Table 2 Design parameters of the collector

Dimensions		1 m×0.5 m×0.12 m (Length × width × thickness)
Pipeline	Spacing between the glass and the plate	30 mm
	Materials	Copper tube
	Arrangement	Serpentine pipeline
	Pipe diameter	24 mm
Glass cover	Pipe spacing	80 mm
	Materials	Low iron ultra-white glass
	Transmittance	92%
	Reflectivity	4%
	Emissivity	10%
Absorber plate	Thickness	4 mm
	Thermal Conductivity	0.76 W/(m·K)
	Materials	Blue titanium heat absorption coating
Insulation	Absorption rate	95%
	Thickness	0.4 mm
	Materials	Phenolic foam
	Thickness	40 mm

## 2.2 Experimental system setup

The indoor experimental system of PCM collector is established and as illustrated in Fig. 4. The system mainly includes a dual-PCM collector, an artificial solar simulator, a water tank, a pump, an electromagnetic flowmeter, an air-cooled condenser and several valves. A TRM-PD1 artificial solar simulator was used to provide solar radiation of which the adjustable extent is 600-1200 W/m<sup>2</sup>. The inlet water temperature was regulated by a temperature controller which was connected to a temperature sensor and an electric heater. An air-cooled condenser was used to cool the water heated by the collector. A pump was used to power the system. A magnetic flowmeter installed on the pipeline was used to measure and record the flow.



Fig. 4 Experimental system of a PCM collector

## 2.3 Operating conditions

High-temperature and low-temperature conditions were designed for the PCM collector. The detailed situation was explained as following.

The high-temperature conditions of this experiment simulated the situation of the strong solar

1 radiation as the daytime. In high-temperature conditions, by using the temperature controller, the  
2 inlet water temperature was regulated to 30°C, 50°C, and 70°C. By adjusting the solar simulator,  
3 the solar radiation intensity was set to approximately 770 W/m<sup>2</sup> to make the outlet water  
4 temperature rising until it was stable at the beginning of the operating conditions, then, the solar  
5 simulator was turned off, and under the action of the condenser, the water temperature of the  
6 collector decreased until it was stable.

7 The low-temperature conditions simulated the situation without solar radiation at night.

8 Under low-temperature conditions, the collector was laid in a closed artificial climate chamber  
9 without solar radiation where the ambient temperature was set to 9-10°C to keep the temperature  
10 of the collector low until it was stable. Then, the temperature control was stopped and the door of  
11 the climate chamber was opened to keep the temperature rising.

12 In the above experimental conditions, the mass flow rate per unit collector area was set to  
13 0.02 (kg/s) [26]. Under the same conditions, the collector without PCM was tested and compared  
14 with the PCM collector. In addition, experiments on the positions of the two kinds of PCMs were  
15 performed.

## 16 2.4 Instrumentation

17 In the experiments, the temperatures of the glass cover, absorber plate, PCMs, inlet and outlet  
18 water were recorded using a thermocouple with an accuracy of ±0.2% (i.e., ±1°C), and the  
19 measuring range was -200°C to 200°C. In addition, under high-temperature conditions, the heat  
20 fluxes of the sidewall and bottom of the collector were measured using a heat flux meter with an  
21 accuracy of ±2.0%, and the heat flux meters were connected to a data acquisition instrument with  
22 a measuring range of -1500 to 1500 W/m<sup>2</sup>. Under low-temperature conditions, the heat flux of the

1 glass cover was also measured. An anemometer with an accuracy of  $\pm 5\%$  (i.e.,  $\pm 0.05$  m/s) was  
2 installed at the height of the midpoint of the collector to measure the air velocity, and the  
3 measuring range was 0.05~30 m/s. An automatic temperature recorder with an accuracy of  $\pm 5\%$   
4 was placed near the collector to record the ambient temperature, and the measuring range was 0 to  
5 55°C. A solar radiation meter with an accuracy of  $\pm 5\%$  was located in the same plane as the  
6 glazing surface of the collector, and there was no shielding to the collector; thus the meter can  
7 accurately measure the solar radiation projected on the collector, and the measuring range is  
8 0~2000 W/m<sup>2</sup>. The sampling period for all of the sensors was 30 s. The locations of the sensors  
9 are shown in Fig. 1. To reduce the effect of the environment on the inlet water temperature, the  
10 pipeline from the outlet of water tank to the inlet of collector was shortened as much as possible  
11 and the pipeline of the system was covered with insulation pipe and aluminum foil.

## 12 2.5 Efficiency calculation method and test procedure

13 For the flat plate collector, the instantaneous efficiency can be obtained by the calculation  
14 formula as follows [26]:

$$15 \quad \eta = \frac{q_m c_p (t_o - t_i)}{A_a I} \quad (1)$$

16 where  $t_i$  is the inlet water temperature (°C),  $t_o$  is the outlet water temperature (°C),  $q_m$  is the  
17 mass flow rate of the water (kg/s),  $c_p$  is the specific heat capacity of the water (J/(kg·K)),  $A_a$   
18 is the lighting area of the collector (m<sup>2</sup>), and  $I$  is the intensity of the solar radiation projected on  
19 the collector (W/m<sup>2</sup>).

20 During the indoor efficiency test experiment of the PCM collector in steady state, the  
21 collector was adjusted with respect to the solar simulator so that the solar radiation projected on  
22 the flat plate collector was vertically incident, and four evenly spaced inlet water temperature

1 conditions (30°C, 40°C, 50°C and 60°C) were selected in the operating temperature range of the  
 2 collector. The measurement process was divided into two phases: 12-minute preparation period  
 3 and 12-minute steady-state measurement period. After a 12-minute preparation period, the system  
 4 arrived in a steady state and the data record was started. The entire measurement process lasted for  
 5 12 minutes, and the average of the measured parameters within 12 minutes was taken for the  
 6 efficiency calculation.

7 The instantaneous efficiency fitting curve of the collector is a linear fitting curve of the  
 8 efficiency based on the lighting area and the inlet water temperature of the collector and should be  
 9 fitted by at least four efficiency points. The formula is as follows:

$$\eta_a = \eta_{0,a} - UT_i^* \tag{2}$$

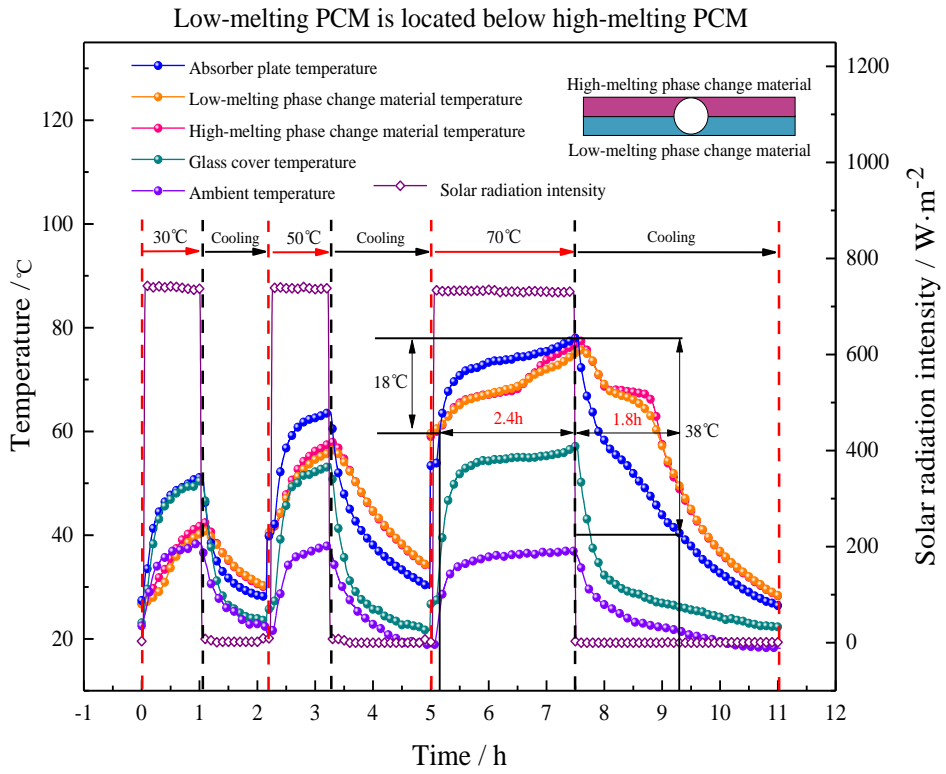
11 where  $T_i^* = (t_i - t_a) / I$  is the normalized temperature difference based on the inlet temperature  
 12  $((m^2 \cdot K) / W)$ ;  $t_a$  is the ambient temperature (°C);  $\eta_{0,a}$  is the instantaneous efficiency intercept  
 13 based on the lighting area and inlet temperature of the collector, which mainly depends on the  
 14 optical characteristics of the glass cover, the absorber and the number of cover layers, and the  
 15 value of this variable indicates the highest efficiency that the collector can theoretically achieve;  
 16 the slope  $U$  is the heat loss coefficient of collector with respect to  $T_i^*$ , which mainly depends  
 17 on the configuration and thermal insulation performance of the collector.

### 19 3. Experimental results

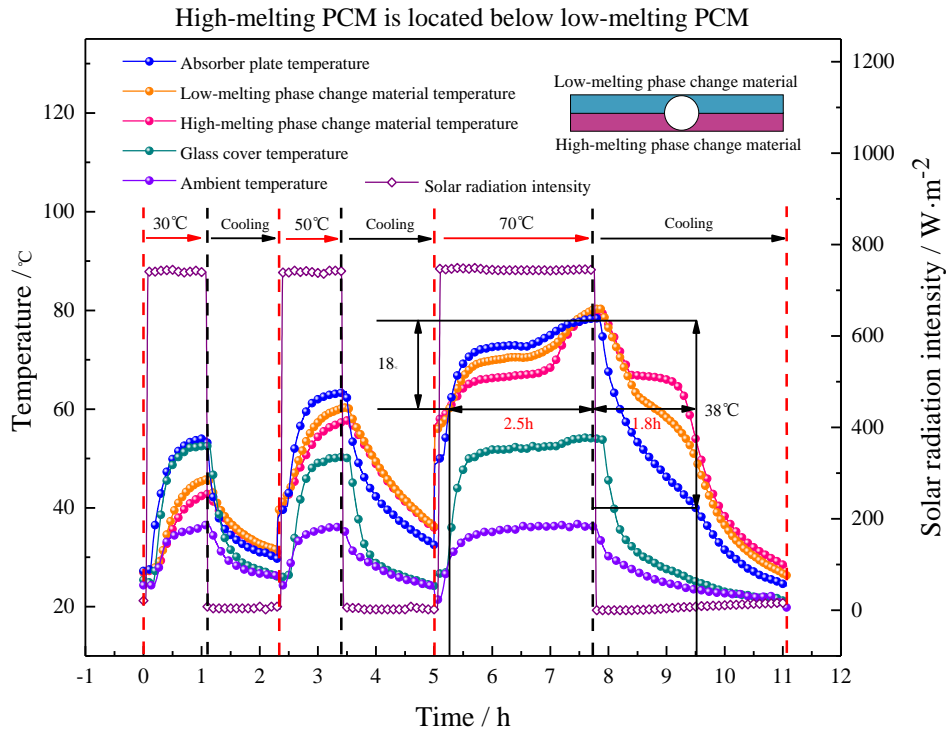
#### 20 3.1 Temperature and heat flux under high-temperature conditions

21 The temperatures of measuring points in the PCM collector and conventional collector for  
 22 various water temperatures in high-temperature conditions are shown in Fig. 5, and the heat fluxes

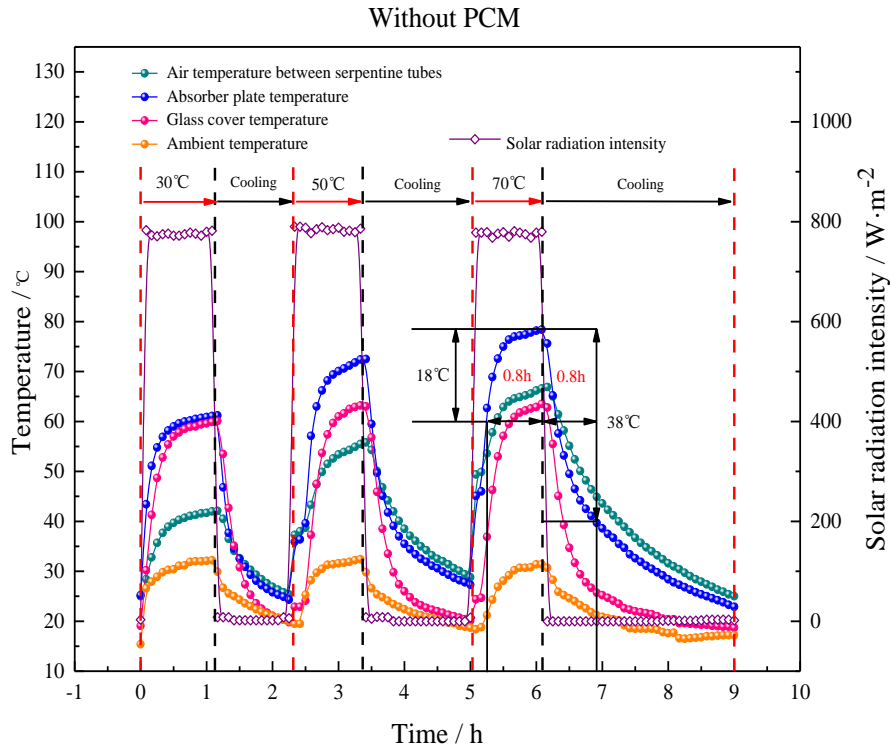
1 of sidewall and bottom are shown in Fig. 6.



3 (a) Low-melting PCM underneath the high-melting PCM



(b) High-melting PCM underneath the low-melting PCM



(c) Without PCM

Fig.5 Temperatures of the measuring points in the collector under high-temperature conditions

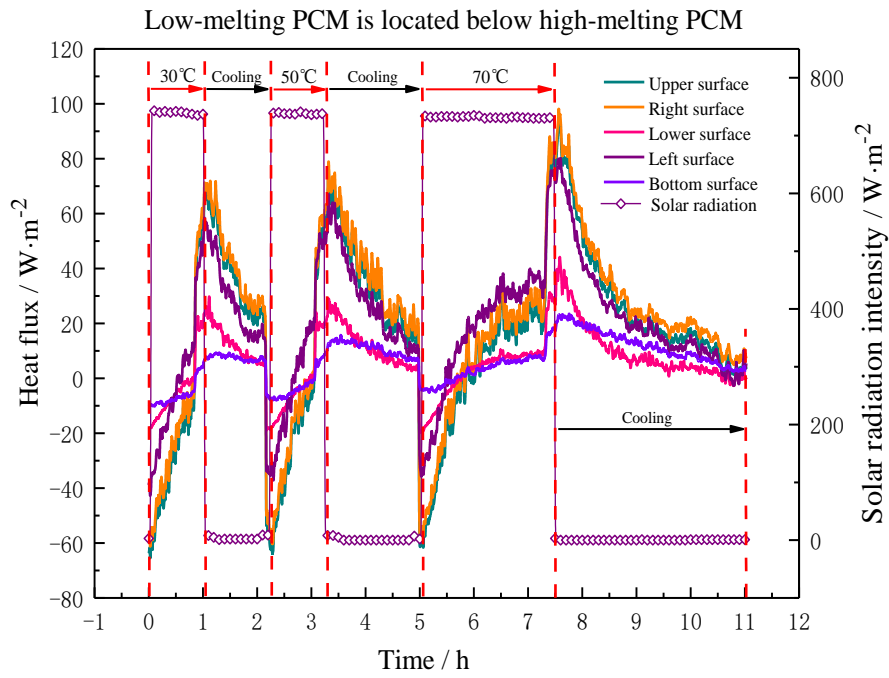
It can be seen from Fig. 5 that in the case of 30°C and 50°C water temperature conditions, after solar simulator was switched on, the temperature of absorber, glass cover and PCMs in all cases ((a), (b) and (c)) increased rapidly within approximately 1 h and then tended to stabilize. After solar simulator was switched off, the temperature dropped rapidly. For the collector without PCM (case (c)), the temperature change under 70°C water temperature condition was similar to that under 30°C and 50°C water temperature conditions. However, for the collector with PCM (case (a) and (b)) and subjected to a 70°C water temperature condition, after the solar radiation was turned on, the temperature of the PCMs and the absorber plate increased rapidly within 0.5 h, then the temperature of the high-melting PCM reached the melting point and the temperature curves of absorber plate and low-melting PCM tended to flatten due to the melting of the

1 high-melting PCM. After all the high-melting PCM was melted, the temperature of the absorber  
2 and PCMs increased rapidly again and tended to stabilize. After the solar simulator was turned off,  
3 the temperature curves of the absorber and PCM dropped rapidly within 0.5 h; then the  
4 high-melting PCM began to solidify and release heat because the temperature reached the freezing  
5 point, the temperature tended to stabilize. Meanwhile, the temperature decrease rate of the  
6 absorber and low-melting PCM was lowered. After all the high-melting PCM was solidified, the  
7 temperature curves of the absorber plate and the PCMs began to drop rapidly again.

8 Moreover, as shown in Fig. 5, it took 2.4 h, 2.5h and 0.8 h for the absorber plate temperature  
9 to increase from 60°C to 78°C for the case (a), (b) and (c), respectively, and it took 1.8 h, 1.8h and  
10 0.8 h for the absorber plate temperature to decrease from 78°C to 40°C, respectively. According to  
11 the time comparison, it can be found that the time taken for the heating and cooling process of the  
12 PCM collector was significantly longer than that of the conventional collector, which mainly  
13 occurred because the high-melting PCM absorbed heat during melting and released heat during  
14 solidification. The time taken for the heating process of the case (b) was slightly longer than that  
15 of the case (a) because the thermal resistance between the absorber plate and the high-melting  
16 PCM was larger when the high-melting PCM is located below the low-melting PCM. However,  
17 the time difference between the case (a) and (b) was small due to the high thermal conductivity of  
18 the PCMs.

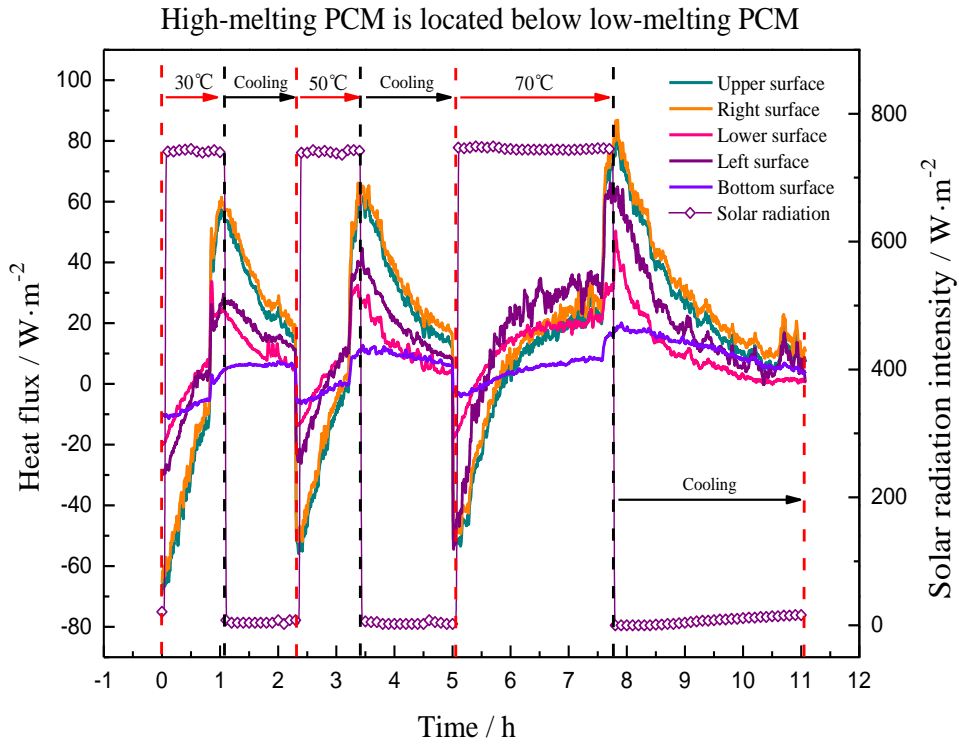
19 It can be seen from the above-mentioned analytical result that the high-melting PCM can  
20 store heat when the high water temperature of the pipe leads to the high-melting PCM melting,  
21 and the time when the temperature reaches the maximum is delayed, thus decrease the temperature  
22 rising rate of the collector and relieving overheating. When the water temperature of the collector

1 decreases with the reduction of solar radiation, the accumulation of heat in the high-melting PCM  
 2 can be used to decrease the temperature drop rate of the collector, thereby improving the thermal  
 3 performance of the collector in low or no solar radiation conditions. In addition, when the  
 4 high-melting PCM is located below the low-melting PCM, the delay effect of the high-melting  
 5 PCM on the time when the temperature reaches the maximum is more obvious.



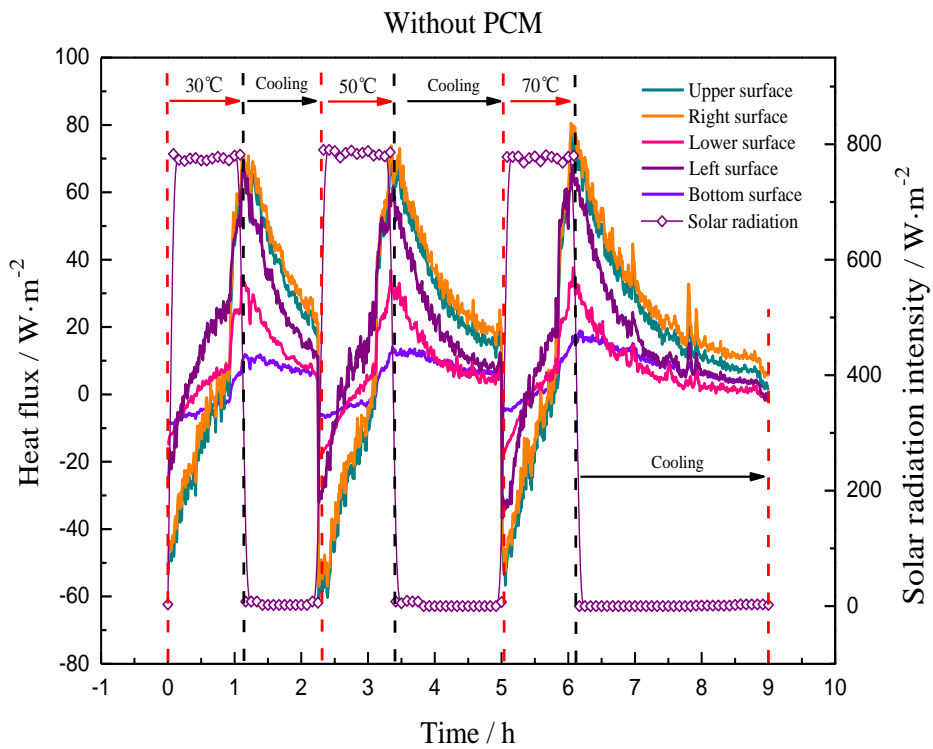
Heat flux: The heat flux transferred from the collector to the environment is positive.

(a) Low-melting PCM is located below the high-melting PCM



1  
2  
27  
28  
29  
30  
31  
32  
33  
34  
35  
36  
37  
38  
39  
40  
41  
42  
43  
44  
45  
46  
47  
48  
49  
50  
51  
52  
53  
54  
55  
56  
57  
58  
59  
60  
61  
62  
63  
64  
65

(b) High-melting PCM is located below the low-melting PCM



3  
4  
56  
57  
58  
59  
60  
61  
62  
63  
64  
65

(c) Without PCM

Fig. 6 Heat flow variations in the PCM collector in high-temperature conditions

1  
2  
3  
4  
5  
6  
7  
8  
9  
10  
11  
12  
13  
14  
15  
16  
17  
18  
19  
20  
21  
22  
23  
24  
25  
26  
27  
28  
29  
30  
31  
32  
33  
34  
35  
36  
37  
38  
39  
40  
41  
42  
43  
44  
45  
46  
47  
48  
49  
50  
51  
52  
53  
54  
55  
56  
57  
58  
59  
60  
61  
62  
63  
64  
65

1  
2       As shown in Fig. 6, under the water temperature conditions of 30 °C and 50°C, after solar  
3 simulator was switched on, as the temperature of collector increased, the heat fluxes transferred  
4 from the collector to the environment changed from negative to positive and increase until the  
5 solar radiation was turned off. Meanwhile, the variation trend of the heat fluxes of the  
6 conventional collector was similar to that of the PCM collector.

7       The heat fluxes changed from negative to positive until the next experimental condition in  
8 Fig. 6. The reason for this status of the heat fluxes were that the temperature differences between  
9 the sidewall of the collector and ambient temperature and the temperature differences between the  
10 bottom of the collector and ambient temperature were relatively low at the beginning period when  
11 the solar simulator was switched on. Then the radiant heat of the collector wall from the solar  
12 simulator was much greater than the convective heat conduction with the air. The overall heat flux  
13 transferred from the environment to the collector. When the temperature of the collector gradually  
14 rose to a stable state, the wall temperature of the collector was much larger than the ambient  
15 temperature. Then the convective heat conduction between the wall and the environment was in  
16 the dominant position, and the overall heat flux transferred from the collector to the environment.

17       Under the water temperature condition of 70 °C, the heat fluxes of the sidewall and bottom of  
18 the PCM collector increased slowly in the melting process of the high-melting PCM. During the  
19 solidification process, as the temperature of the collector gradually decreased and was close to the  
20 environment temperature, the heat fluxes of the collector approached zero, and the trend of heat  
21 fluxes dropping slowly was not obvious; however, compared with the conventional collector, the  
22 time had been prolonged. The above analysis shows that when the high water temperature of pipe

1 leads to the high-melting PCM melting, the high-melting PCM can slow the heat absorption of  
2 collector, and when water temperature drops, the accumulation of heat in the PCM can be  
3 effectively utilized to slow the heat dissipation process of the collector.

### 5 **3.2 Temperature and heat flux under low-temperature conditions**

6 The temperatures of the measuring points in the PCM collector and conventional collector  
7 under low-temperature conditions are shown in Fig. 7, and the heat fluxes of the sidewall, bottom  
8 and glass cover are shown in Fig. 8.

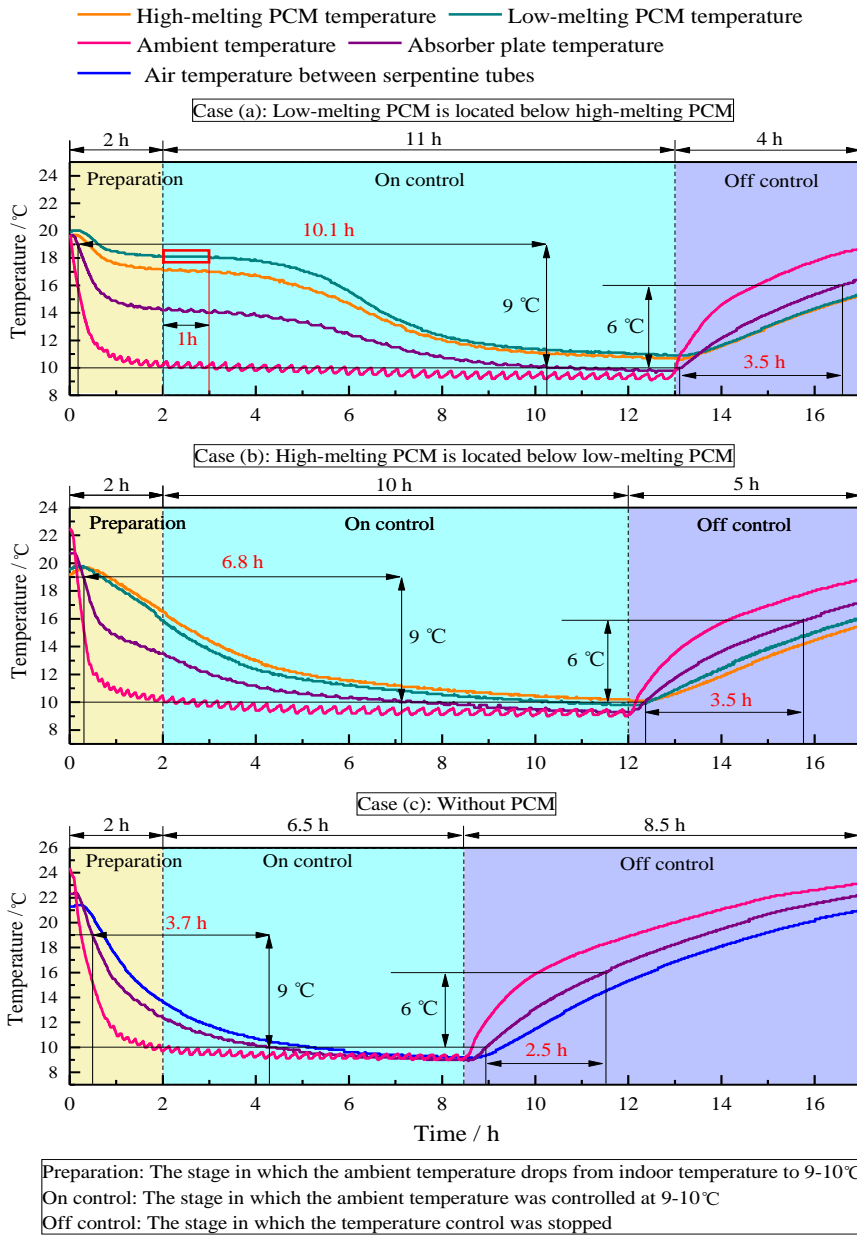


Fig. 7 Temperature variations in the PCM collector under low-temperature conditions

As shown in Fig. 7, compared with the collector without PCM, when the low-melting PCM was located below high-melting PCM, the temperature of PCMs and absorber was lowered rapidly with the decrease of the ambient temperature at the beginning. After that, the temperature curves dropped slowly because the temperature of the low-melting PCM decreased to the freezing point and the low-melting PCM began to solidify and release heat. At the same time, there was an

1 obvious one-hour constant temperature interval for the low-melting PCM, which indicates that the  
2  
3 low-melting PCM can obviously slow the temperature decrease rate of absorber and relieve the  
4  
5 freezing problem of flat plate collector in the low-temperature environment. There was a tendency  
6  
7 to drop slowly for the temperature curve of absorber when the high-melting PCM was located  
8  
9 below low-melting PCM. However, the constant temperature interval did not exist in the  
10  
11 temperature curve of the low-melting PCM, it can be mainly interpreted as the low-melting PCM  
12  
13 located above the high-melting PCM was greatly affected by the environment temperature,  
14  
15 resulting in a fast phase change. On the contrary, compared with the conventional collector, the  
16  
17 temperature of the PCM collector decreased more slowly.  
18  
19  
20  
21  
22  
23  
24

25 As shown in Fig. 7, it took 10.1 h, 6.8 h and 3.7 h for the absorber plate temperature to  
26  
27 decrease from 19°C to 10°C for the case (a), (b) and (c), respectively, this indicates that the time  
28  
29 taken for the cooling process can be prolonged by the solidification exotherm of the low-melting  
30  
31 PCM. When the temperature control was stopped, as the environment temperature increased, the  
32  
33 temperature of the collector gradually increased. As shown in Fig. 7, it took 3.5 h, 3.5 h and 2.5 h  
34  
35 for the absorber plate temperature to increase from 10°C to 16°C for the case (a), (b) and (c),  
36  
37 respectively, which shows that the time taken for the temperature rising process of the PCM  
38  
39 collector is longer because of the heat absorption of low-melting PCM during the melting process.  
40  
41  
42  
43  
44  
45  
46  
47  
48  
49  
50  
51  
52  
53  
54  
55  
56  
57  
58  
59  
60  
61  
62  
63  
64  
65

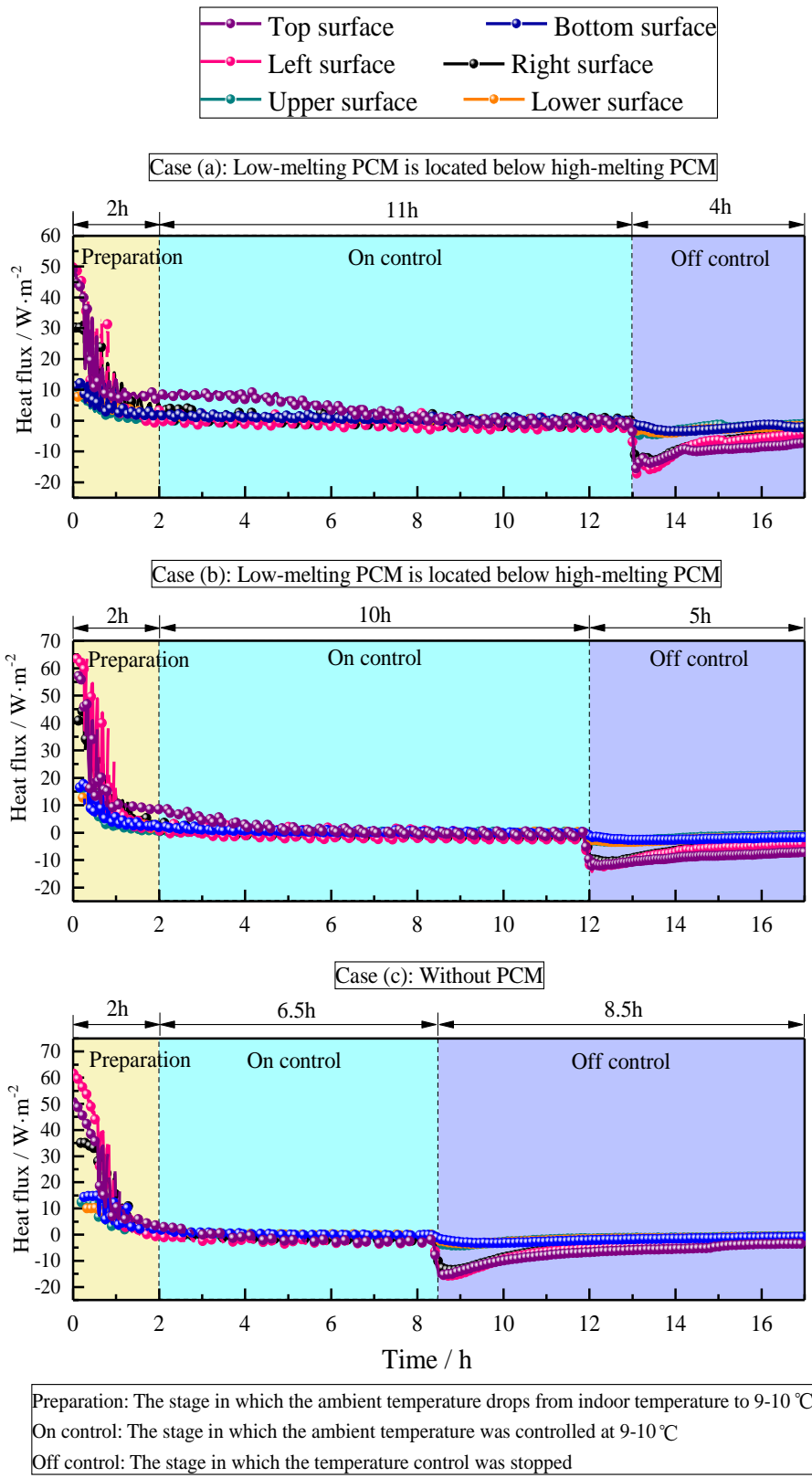


Fig. 8 Heat flow variations in the PCM collector under high-temperature conditions

1 It can be seen from Fig. 8 that the heat fluxes of the sidewall and the bottom of the collector  
2 decreased rapidly with decreasing air temperature and quickly approached zero for the case (a), (b)  
3 and (c), which shows that the temperatures of the sidewall and the bottom are close to the  
4 environment temperature, and the heat exchange between them approaches zero at this time.  
5 Furthermore, the heat flux of the glass cover tended to stabilize within two hours after the second  
6 hour when the low-melting PCM was located below the high-melting PCM (case (a)). Even  
7 though there was an increasing trend in the middle of the process, indicating that the temperature  
8 of the air layer in the PCM collector was higher than the environment temperature due to the heat  
9 release of the low-melting PCM during solidification. All of these properties are beneficial to the  
10 antifreeze performance of the collector. When the high-melting PCM was located below the  
11 low-melting PCM (case (b)), the trend of the heat flux decreasing slowly was less obvious, but the  
12 time when the heat flux of the glass cover dropped to zero was still delayed. When the door of the  
13 climate chamber was opened and the ambient temperature increased rapidly, the heat fluxes  
14 quickly dropped from zero to a negative value and then slowly increased and approached zero, and  
15 the duration of this process of the PCM collector was substantially longer than that of the  
16 conventional collector. According to the comprehensive analysis of temperature and heat flow, the  
17 following conclusion can be drawn: placing the low-melting PCM below the high-melting PCM  
18 provided the greatest frost resistance to the collector.

## 20 **4. Discussion and analysis**

### 21 **4.1 Time analysis**

22 Compared with the conventional collector, in the 70°C water temperature condition, the time

1 taken for the temperature of the absorber plate to increase from 60°C to 78°C could be prolonged  
2  
3 by 1.6 h and 1.7 h for the case (a) and case (b), respectively, which could reduce overheating  
4  
5 problems of the collector. The time taken for the temperature of the absorber plate to decrease  
6  
7 from 78°C to 40°C could be prolonged by 1 h for the case (a) and case (b), which indicates that  
8  
9 the heat stored in the high-melting PCM can be effectively used to enhance the thermal  
10  
11 performance during the cooling process. According to the time comparison, the prolonged time  
12  
13 was longer when the high-melting PCM was located below the low-melting PCM, but the  
14  
15 difference was not significant.  
16  
17  
18  
19  
20  
21

22 Under a 9-10°C low-temperature environment, the time taken for the temperature of the  
23  
24 absorber plate to decrease from 19°C to 10°C could be prolonged by 6.4 h and 3.1 h for the case  
25  
26 (a) and (b), respectively, which can reduce freezing problems of the collector. According to the  
27  
28 time comparison, when the low-melting PCM was located below the high-melting PCM, the  
29  
30 antifreeze effect of the PCM on the collector was more substantial.  
31  
32  
33  
34  
35  
36  
37  
38

#### 39 4.2 Efficiency analysis

40  
41 According to the efficiency calculation method, the efficiencies of the collector were  
42  
43 calculated in the four inlet water temperature conditions (30°C, 40°C, 50°C and 60°C), and the  
44  
45 efficiency curves of the PCM collector and conventional collector were obtained and compared, as  
46  
47 shown in Fig. 9. Both the PCM collector and the collector without PCM exhibited lower collector  
48  
49 efficiency, mainly because the collector was assembled by the experimenter and had low sealing  
50  
51 performance, which resulted in the large heat loss. However, the effect of PCMs on the efficiency  
52  
53 of the collector can still be reflected by comparing the relative values of different efficiencies.  
54  
55  
56  
57  
58  
59  
60  
61  
62  
63  
64  
65

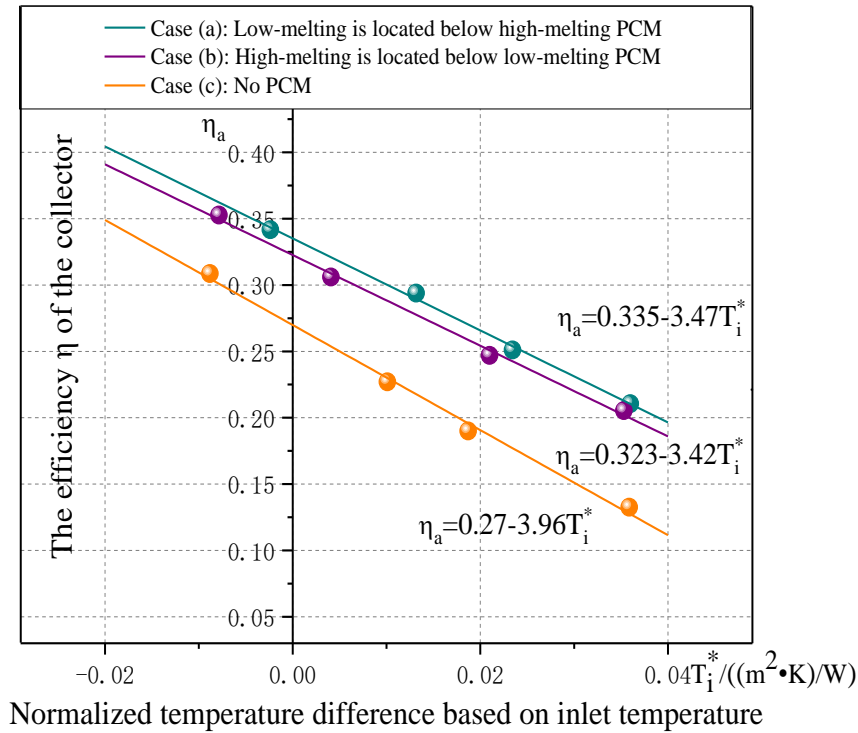


Fig. 9 Efficiencies of the PCM collector and conventional collector

As shown in Fig. 9, the efficiency of the PCM collector was higher than that of the collector without PCM, and the efficiency of the PCM collector in case (a) and case (b) was increased by 24.1% and 19.6% compared with that of the traditional collector, respectively. The increased efficiency mainly occurs because the absorber plate bottom of the PCM collector and that of the collector without PCM were filled with PCM and air respectively. The thermal conductivity of the PCM was better than that of the air. Moreover, the efficiency test of the PCM collector was carried out under steady conditions [26]. As a result, the PCM of the collector was not in the phase change period. Therefore, the thermal resistance between the absorber plate and the pipe was reduced. The efficiency of the PCM collector was increased.

## 5. Conclusions

1 In this study, a new dual-PCM collector was proposed that can relieving the freezing and  
2 overheating problems of a flat plate collector, and experiments were conducted to study the heat  
3 transfer process and thermal performance of the dual-PCM collector; the efficiency of the  
4 dual-PCM collector was then compared to that of a traditional collector. The research obtains the  
5 following detailed conclusions:

6 (1) In the case of high water temperature, the high-melting PCM in the PCM collector can  
7 decrease the temperature rising rate of the collector by melting and absorbing heat. The time  
8 taken for the temperature of the absorber plate to rise from 60 °C to 78 °C can be prolonged  
9 by 1.6 h and 1.7 h when the low-melting PCM placed below the high-melting PCM and in  
10 the opposite condition, which can relieve overheating problems of the collector. When the  
11 water temperature is lowered, the excess heat stored by the high-melting PCM can be  
12 effectively utilized to enhance the thermal performance of the collector. The heat fluxes of  
13 sidewall and bottom also increase slowly due to the melting of the high-melting PCM in the  
14 heating process.

15 (2) In the case of low temperature, the low-melting PCM of the PCM collector can solidify and  
16 release heat to substantially slow the cooling of the collector. When the low-melting PCM  
17 placed below the high-melting PCM and in the opposite condition, the time taken for the  
18 temperature of the absorber plate to decrease from 19°C to 10°C could be prolonged by 6.4 h  
19 and 3.1 h, respectively, thereby relieving the freezing problems of the collector. During the  
20 exothermic solidification of the low-melting PCM, the temperature of the air layer is higher  
21 than the ambient temperature, which is beneficial to the antifreeze of the collector.

22 (3) Compared with a conventional collector, the efficiency of the PCM collector when placing

1 the low-melting PCM below the high-melting PCM and in the opposite condition is increased  
2  
3  
4 by 24.1% and 19.6%, respectively.  
5  
6  
7  
8

#### 9 **References**

- 10  
11 [1] Y. Liu, Y. Zhou, Y. Chen, et al. Comparison of support vector machine and copula-based  
12 nonlinear quantile regression for estimating the daily diffuse solar radiation: A case study in  
13  
14 China. *Renewable Energy*, 2020, 146: 1101-1112.  
15  
16  
17  
18  
19 [2] D. Wang, Q. Gao, Y. Liu, et al. Experimental study on heating characteristics and parameter  
20 optimization of transpired solar collectors. *Applied Energy*, 2019, 238: 534–546.  
21  
22  
23  
24 [3] S. Harrison, C. A. Cruickshank A review of strategies for the control of high temperature  
25 stagnation in solar collectors and systems. *Energy Procedia*, 2012, 30:793-804.  
26  
27  
28  
29 [4] B. A. Wilcox, C. S. Barnaby. Freeze protection for flat-plate collectors using heating. *Solar*  
30  
31  
32  
33  
34  
35  
36  
37 [5] L. Crofoot, S. Harrison. Performance Evaluation of a Liquid Desiccant Solar Air  
38  
39  
40  
41  
42  
43  
44  
45  
46  
47  
48  
49  
50  
51 [6] H. Kessentini, J. Castro, R. Capdevila, et al. Development of flat plate collector with plastic  
52  
53  
54  
55  
56  
57  
58  
59  
60  
61  
62  
63  
64  
65

- 1 [8] [S. Hussain, S. J. Harrison](#). Evaluation of thermal characteristics of a flat plate Solar Collector  
2 with a back mounted air channel. [Applied Thermal Engineering](#), 2017, 123:940-952.
- 3 [9] [A. C. Gladen, J. H. Davidson, S. C. Mantell](#). Selection of thermotropic materials for overheat  
4 protection of polymer absorbers. [Solar Energy](#), 2014, 104:42-51.
- 5 [10] [K. Resch, G. M. Wallner](#). Thermotropic layers for flat-plate collectors—A review of various  
6 concepts for overheating protection with polymeric materials. [Solar Energy Materials and](#)  
7 [Solar Cells](#), 2009, 93(1):119-128.
- 8 [11] [G. M. Wallner, K. Resch, R. Hausner](#). Property and performance requirements for  
9 thermotropic layers to prevent overheating in an all polymeric flat-plate collector. [Solar](#)  
10 [Energy Materials and Solar Cells](#), 2008, 92(6):614-620.
- 11 [12] [D. R. Koenigshofer](#). Freeze protection for solar collectors. [Sunworld](#), 1977.
- 12 [13] [Y. Wei, W. Xi, J. Yuan, et al](#). The antifreeze mechanism of flat plate-type solar collector and  
13 material characteristics of absorber plate// [The New Solar Energy Technology in the 21st](#)  
14 [Century: the Monograph of Academic Annual Conference](#). Shanghai: Shanghai Jiaotong  
15 University Press, 2003: 407-410.
- 16 [14] [X. Jiang, Z. Tao, J. Lu, et al](#). Theoretical and experimental studies on sequential freezing  
17 solar water heater. [Solar Energy](#), 1994, 53(2):139-146.
- 18 [15] [A. Ozsoy, S. Demirer, N. M. Adam](#). An Experimental Study on Double-Glazed Flat Plate  
19 Solar Water Heating System in Turkey. [Applied Mechanics and Materials](#), 2014,  
20 564:204-209.

- 1 [16] K. S. Reddy, N. D. Kaushika. Comparative study of transparent insulation materials cover  
2 systems for integrated-collector-storage solar water heaters. *Solar Energy Materials and Solar*  
3 *Cells*, 1999, 58(4):431-446.
- 4 [17] F. Zhou, J. Jie, J. C, et al. Experimental and numerical study of the freezing process of  
5 flat-plate solar collector. *Applied Thermal Engineering*, 2017, 118: 773-784.
- 6 [18] W. Su, R. Zuo, Z. Zhang, et al. Flat-plate solar collector/storage system. *Acta Energiæ*  
7 *Solaris Sinica*, 2008, 29(4): 449-453.
- 8 [19] A.E. Kabeel, A. Khalil, S.M. Shalaby, et al. Experimental investigation of thermal  
9 performance of flat and v-corrugated plate solar air heaters with and without PCM as thermal  
10 energy storage. *Energy Conversion and Management*, 2016, 113: 264-272.
- 11 [20] Z. Chen, M. Gu, D. Peng. Heat transfer performance analysis of a solar flat-plate collector  
12 with an integrated metal foam porous structure filled with paraffin. *Applied Thermal*  
13 *Engineering*, 2010, 30(14): 1967-1973.
- 14 [21] J. Zhao, Z. Wang, K. Wang, et al. The design and research of anti-freezing solar flat plate  
15 collector with phase change energy storage layer. *Journal of Central South University*  
16 *(Science and Technology)*, 2016, 47(10): 3575-3581.
- 17 [22] A. J. N. Khalifa, K. H. Suffer, M. S. Mahmoud. A storage domestic solar hot water system  
18 with a back layer of phase change material. *Experimental Thermal and Fluid Science*, 2013,  
19 44: 174-181.
- 20 [23] E. B. S. Mettawee, G. M. R. Assassa. Experimental study of a compact PCM solar collector.  
21 *Energy*, 2006, 31(14): 2958-2968.

- 1 [24] E. B. S. Mettawee, G. M. R. Assassa. Thermal conductivity enhancement in a latent heat  
2 storage system. *Solar Energy*, 2007, 81(7): 839-845.
- 3 [25] Y. Varol, A. Koca, H. F. Oztop, et al. Forecasting of thermal energy storage performance of  
4 Phase Change Material in a solar collector using soft computing techniques. *Expert Systems*  
5 with Applications, 2010, 37(4): 2724-2732.
- 6 [26] General Administration of Quality Supervision, Inspection and Quarantine of the People's  
7 Republic of China. "GB/T 4271-2007" Test methods for the thermal performance of solar  
8 collectors. Beijing: China Standard Press, 2007.
- 9 [27] F. Zhou, J. Ji, W. Yuan, et al. Study on the PCM flat-plate solar collector system with  
10 antifreeze characteristics. *International Journal of Heat and Mass Transfer* 129, 357-366, doi:  
11 <https://doi.org/10.1016/j.ijheatmasstransfer.2018.09.114> (2019).
- 12 [28] P. Charvát, L. Klimeš, O. Pech, et al. Solar air collector with the solar absorber plate  
13 containing a PCM – Environmental chamber experiments and computer simulations.  
14 *Renewable Energy* 143, 731-740, doi: <https://doi.org/10.1016/j.renene.2019.05.049> (2019).
- 15

Nomenclature	
$\eta$	Instantaneous efficiency
$t_i$	Inlet water temperature (°C)
$t_o$	Outlet water temperature (°C)
$q_m$	Mass flow of the water (kg/s)
$c_p$	Specific heat capacity of the water (J/(kg·K))
$A_a$	Lighting area of the collector (m <sup>2</sup> )

1  
2  
3  
4  
5  
6  
7  
8  
9  
10  
11  
12  
13  
14  
15  
16  
17  
18  
19  
20  
21  
22  
23  
24  
25  
26  
27  
28  
29  
30  
31  
32  
33  
34  
35  
36  
37  
38  
39  
40  
41  
42  
43  
44  
45  
46  
47  
48  
49  
50  
51  
52  
53  
54  
55  
56  
57  
58  
59  
60  
61  
62  
63  
64  
65

$I$	The intensity of the solar radiation projected on the collector ( $\text{W}/\text{m}^2$ )
$T_i^*$	Normalized temperature difference based on the inlet temperature  $((\text{m}^2 \cdot \text{K})/\text{W})$
$t_a$	Ambient temperature ( $^{\circ}\text{C}$ )
$\eta_{0,a}$	Instantaneous efficiency intercept based on the lighting area and inlet temperature of the collector
$U$	Heat loss coefficient of the collector with reference to $T_i^*$
<b>Subscripts</b>	
$i$	Inlet
$o$	Outlet
$a$	Ambient

1



1 **Abstract:** In order to overcome the freezing and overheating problems of solar collectors, a novel  
2  
3 dual-phase change material (PCM) flat plate collector was proposed in this research. There were  
4  
5 two layers of PCMs in the solar collector, one layer material with a phase change temperature of  
6  
7 70°C and another with a phase change temperature of 15°C, respectively. They were placed in the  
8  
9 space area under the absorber plate in the dual-PCM collector. Frost and High-temperature  
10  
11 resistance performance of the novel dual-phase change material solar collector was tested  
12  
13 systematically in a laboratory. The experimental results show that the high-melting PCM in the  
14  
15 PCM collector can store enough heat and the time taken for the temperature of the absorber plate  
16  
17 to increase from 60 °C to 78 °C could be prolonged by 1.6 h and 1.7 h when low-melting point  
18  
19 PCM placed below high-melting PCM and in the opposite condition. And when the water  
20  
21 temperature decreases, the excess heat stored by the high-melting PCM can be effectively utilized  
22  
23 to improve the thermal performance of the collector under low or no solar radiation conditions.  
24  
25 Under the low-temperature conditions, the low-melting point PCM can substantially slow the  
26  
27 temperature decrease of the collector by solidifying and releasing heat. Moreover, the time taken  
28  
29 for the temperature of the absorber plate to decrease from 19 °C to 10 °C could be prolonged by  
30  
31 6.4 h and 3.1 h when low-melting point PCM placed below high-melting PCM and in the opposite  
32  
33 condition. Thus it can be seen that the dual-PCM collector can significantly overcome the  
34  
35 phenomenon of overheating and freezing. Furthermore, compared with an ordinary flat plate  
36  
37 collector, the efficiency of the dual-PCM collector was increased by 24.1% and 19.6% when  
38  
39 placing low-melting PCM below high-melting PCM and in the opposite condition respectively.  
40  
41  
42  
43  
44  
45  
46  
47  
48  
49  
50  
51  
52  
53  
54  
55

56 **Keywords:** Flat plate solar collector; Frost and High-temperature resistance; Phase change  
57  
58 material; Efficiency; Experimental.  
59  
60  
61  
62  
63  
64  
65

# 1. Introduction

Solar collector is a core component in various solar thermal utilization systems. Its main function is to collect solar radiation energy and transforms heat energy to thermal users by a solid, liquid, or gas medium. In general, solar collectors are mainly divided into the following categories: flat plate collectors, heat pipe collectors, vacuum tube collectors and concentrator collectors. Among these types, flat plate collectors have been extensively used worldwide due to their simple structure, reliable operation, and low cost and favorable solar building integration performance. However, there are also two main drawbacks for flat plate solar collectors: the collector would be overheated in the case of intense solar radiation or with less heat using, and freezing cracks in a low-temperature environment [1-2]. The flat plate solar collector will receive a substantial amount of energy during the sunny days, which can easily lead to pipe fouling and system overheating, especially in the case of heat accumulation. These phenomena can cause pipes to burst and systems to shut down in severe cases. In low-temperature nighttime environments, water—a common circulating fluid used in collectors—can easily freeze and damage the collector, which will affect the operation of the whole system. Therefore, freezing and overheating prevention is essential to extending the service life of a collector and ensuring the stable and reliable operation of a solar collector system.

Currently, overheating problems are mainly handled by the following approaches: application of heat dumps or heat wasters, venting to remove excess heat, and application of the thermotropic layers on the absorber or the glazing. Crofoot L [3] designed a heat waster for the solar collector array that consists of a control and valving system to exhaust excess heat to the atmosphere; however, this heat waster is expensive. Kessentini H [4] proposed a low-cost anti-overheating

1 collector in which a thermally actuated door installed on the flow channel of the collector is used  
2  
3 to ventilate and prevent the collector from overheating in stagnation conditions and this system  
4  
5 can be used to supply the heat from 80 to 120 °C. Gladen A C [5-6] studied the passive air  
6  
7 cooling of flat plate collectors to solve overheating problems in stagnation conditions, and the  
8  
9 results show that the stagnation temperature 170 °C can be decreased to the normal temperature  
10  
11 range. Thermotropic material is a unique material of which the transmission properties change  
12  
13 with respect to the temperature, and some researchers [7-9] have studied the application of  
14  
15 thermotropic layers on the glass over and absorber plate of flat plate collectors to provide passive  
16  
17 overheat protection. The methods described above either eliminate the excess heat obtained by the  
18  
19 collectors or reduce the solar energy collected, which would lead to a lot of waste of energy.  
20  
21  
22  
23  
24  
25  
26  
27

28 Freezing problems of the collectors are mainly handled by using the following approaches:  
29  
30 operation adjustment of the system, special design of the flow channel, and reduction of heat loss  
31  
32 in the collector. D. R. Koenigshofer [10] summarized the methods of freeze protection for solar  
33  
34 collectors, including the emptying method, reverse circulation method, and adding antifreeze  
35  
36 liquid. Yikang W [11] designed a special diamond flow channel which was made of ferritic  
37  
38 stainless steel material to accommodate the expanded volume of water frozen. Xinian J [12] used  
39  
40 rubber for the upper and lower headers and circulation pipes of solar water heaters and used  
41  
42 high-efficiency copper-aluminum composite strips for the discharge pipes to realize a freezing  
43  
44 sequence of the pipes from the center to the ends according to the theory of sequential freezing,  
45  
46 and the solar water heater can operate normally without other auxiliary equipment. Some  
47  
48 researchers investigated the double glass-cover and the transparent insulation material (TIM) to  
49  
50 lower the heat loss of collectors used in extremely cold areas. Ozsoy A [13] conducted an  
51  
52  
53  
54  
55  
56  
57  
58  
59  
60  
61  
62  
63  
64  
65

1 experimental study to a double-glazed flat plate collector and found that the efficiency can be  
2 increased by 24% when the temperature a difference between the water and the environment is 40  
3 °C. Reddy K S [14] studied the effect of different configuration of TIM on the heat loss reduction  
4 of the collector. Zhou F [15, 25] conducted a numerical investigation to the antifreeze  
5 performance of the collector with TIM transparent honeycomb, and the results indicated that the  
6 frozen time could be delayed by 2.5 h. However, these methods would lead to a high cost,  
7 complicate the structure, or reduce the thermal performance of the collector.

8 A phase change material (PCM) can change its physical state by melting and solidifying  
9 within a particular temperature range. And in the process of melting or solidification, the  
10 temperature of a PCM remains approximately constant, which forms a constant temperature  
11 interval for a period of time, and the latent heat absorbed or released is quite large. Therefore, a  
12 PCM can be combined with a flat plate collector to change the heat transfer process of collector  
13 and optimize the corresponding frost resistance and high-temperature resistance.

14 Over the past two decades, a large number of researches have investigated PCM solar  
15 collectors. Su [16] added a layer of 5 cm thick inorganic PCM between the absorber and the  
16 insulation of the collector to increase the collector efficiency by 36%. AEKabeel [17] conducted a  
17 study on a PCM (paraffin) air collector with different absorber plates (flat plate and v-corrugated  
18 plate) by experiments, and found that v-corrugated solar collector had a better thermal  
19 performance than the traditional collector with or without PCM, and the v-corrugated collector  
20 with PCM had a 12% higher daily efficiency than that without PCM. Chen [18] designed a  
21 paraffin solar collector wherein the solar energy received by the collector was stored in paraffin in  
22 the form of heat in the day, and the heat is transferred to the working medium by capillary tubes

1 located inside the paraffin during the nighttime. Zhao Jing [19] proposed a PCM flat plate  
2 collector; the solidifying point of their PCM was 277.15~281.15 K, and their simulation results  
3 indicated that at the lowest temperature in winter, the minimum temperature of the water was  
4 higher than 275.15 K, which can achieve an antifreeze effect. Khalifa AJN [20] integrated a heat  
5 storage container with solar collector. The back of collector was connected with a container  
6 containing the paraffin as a heat storage medium. The study found that the water of the pipe can be  
7 continuously heated after sunset because of the melting exotherm of the PCM. Mettawee EBS et  
8 al. [21-22] experimentally investigated a compact PCM collector and analyzed the heat transfer  
9 characteristics in the melting and solidification process, and their results showed that the useful  
10 heat can be increased by increasing flow rate and adding the aluminum powder to the PCM. Varol  
11 Y [23] experimentally studied a PCM collector using  $\text{NaCO}_3 \cdot \text{H}_2\text{O}$  as the PCM and found that the  
12 useful energy and efficiency of the collector can be enhanced by adding of PCM and the  
13 efficiency increased even solar radiation was reduced. Charvát P [26] compared sheet metal  
14 collector with the collector composed of nine aluminium plates containing a paraffin-based PCM  
15 (Rubitherm RT 42). Both computer simulations and experimental data show that latent heat  
16 thermal energy storage can effectively lower the fluctuations of outlet air temperature as the solar  
17 radiation intensity changes rapidly, e.g. on cloudy days, but the energy efficiency of the PCM  
18 collector was lower than that of the sheet metal collector. The above studies mainly used PCMs of  
19 a specific melting point to store heat in the daytime and release heat in the nighttime, which  
20 integrates heat collection with heat storage to enhance the thermal performance of the collector  
21 after sunset. However, studies that solve frost cracking or overheating problems of flat plate  
22 collectors using PCM have rarely been reported in the literature.

1           The freezing and overheating problems of the flat plate collector have a severe impact on the  
2  
3           normal working of the collector and the stability of the solar water heating system. However, for  
4  
5  
6           the traditional solution, there are problems such as complicated structure, waste of energy and so  
7  
8  
9           on. In addition, it is difficult to apply the traditional method in the case which there are both  
10  
11           cracking and overheating problems during long-term operation of the collector. PCM can absorb  
12  
13  
14           heat when melting and release heat when solidifying. Therefore, applying a layer of high-melting  
15  
16  
17           PCM and a layer of low-melting PCM simultaneously to the collector can alleviate the frost  
18  
19  
20           cracking and overheating problems of the flat plate collector, meanwhile, it avoids the waste of  
21  
22  
23           excess energy and does not increase the complexity of the structure of the collector.  
24

25           To solve the problems of plate collectors (freezing cracks under low-temperature  
26  
27  
28           environments and overheating under strong radiation environments), this paper proposes a  
29  
30  
31           dual-PCM flat plate collector. The collector contains two layers of PCMs with different melting  
32  
33  
34           points of 70°C and 15°C which placed under the absorber plate to relieve the freezing and  
35  
36  
37           overheating problems of the collector. The experiments were performed to investigate the heat  
38  
39  
40           transfer process and the efficiency of the PCM collector. The delay effect of the PCMs on the  
41  
42  
43           highest and lowest temperature point of the collector was researched by comparing the  
44  
45  
46           temperature and heat fluxes of the conventional and PCM collectors, and the thermal performance  
47  
48           improvement of the PCMs on the collector is studied through the efficiency calculation.  
49

## 50           19 51 52 53           20   **2. Methodology**

### 54 55           21   **2.1 PCM collector design**

56  
57  
58           22           The structure of the proposed PCM collector is shown in Fig. 1, and the image of the PCM  
59  
60  
61  
62  
63  
64  
65

1 collector is shown in Fig. 2. An s-shaped pipe is located below the absorber plate, and two kinds  
2  
3 of PCMs (a “high-melting PCM” with a phase change temperature of 70°C and a “low-melting  
4  
5 PCM” with a phase change temperature of 15°C) wrapped with aluminum foil are placed in the  
6  
7 space area under the absorber plate, respectively. Under intense radiation, high-temperature  
8  
9 environment, when the water temperature causes the high-melting PCM temperature to exceed  
10  
11 70°C, the PCM will melt and absorb heat to protect the working fluid from overheating. In a  
12  
13 low-temperature condition, when the temperature of the low-melting PCM is less than 15°C, the  
14  
15 PCM will solidify and release heat to protect the working fluid from freezing. The experiment  
16  
17 chose a kind of high thermal conductivity PCM that is encapsulated in spherical particles and  
18  
19 maintains a solid form after melting, and the PCM is made of high-purity graphite and natural  
20  
21 grease. A picture and the physical parameters of the spherical particle PCMs are shown in Fig. 3  
22  
23 and Table 1, respectively. The specific design parameters of the PCM collector are listed in Table  
24  
25  
26  
27  
28  
29  
30  
31  
32  
33  
34 2.  
35  
36  
37  
38  
39  
40  
41  
42  
43  
44  
45  
46  
47  
48  
49  
50  
51  
52  
53  
54  
55  
56  
57  
58  
59  
60  
61  
62  
63  
64  
65

1  
2  
3  
4  
5  
6  
7  
8  
9  
10  
11  
12  
13  
14  
15  
16  
17  
18  
19  
20  
21  
22  
23  
24  
25  
26  
27  
28  
29  
30  
31  
32  
33  
34  
35  
36  
37  
38  
39  
40  
41  
42  
43  
44  
45  
46  
47  
48  
49

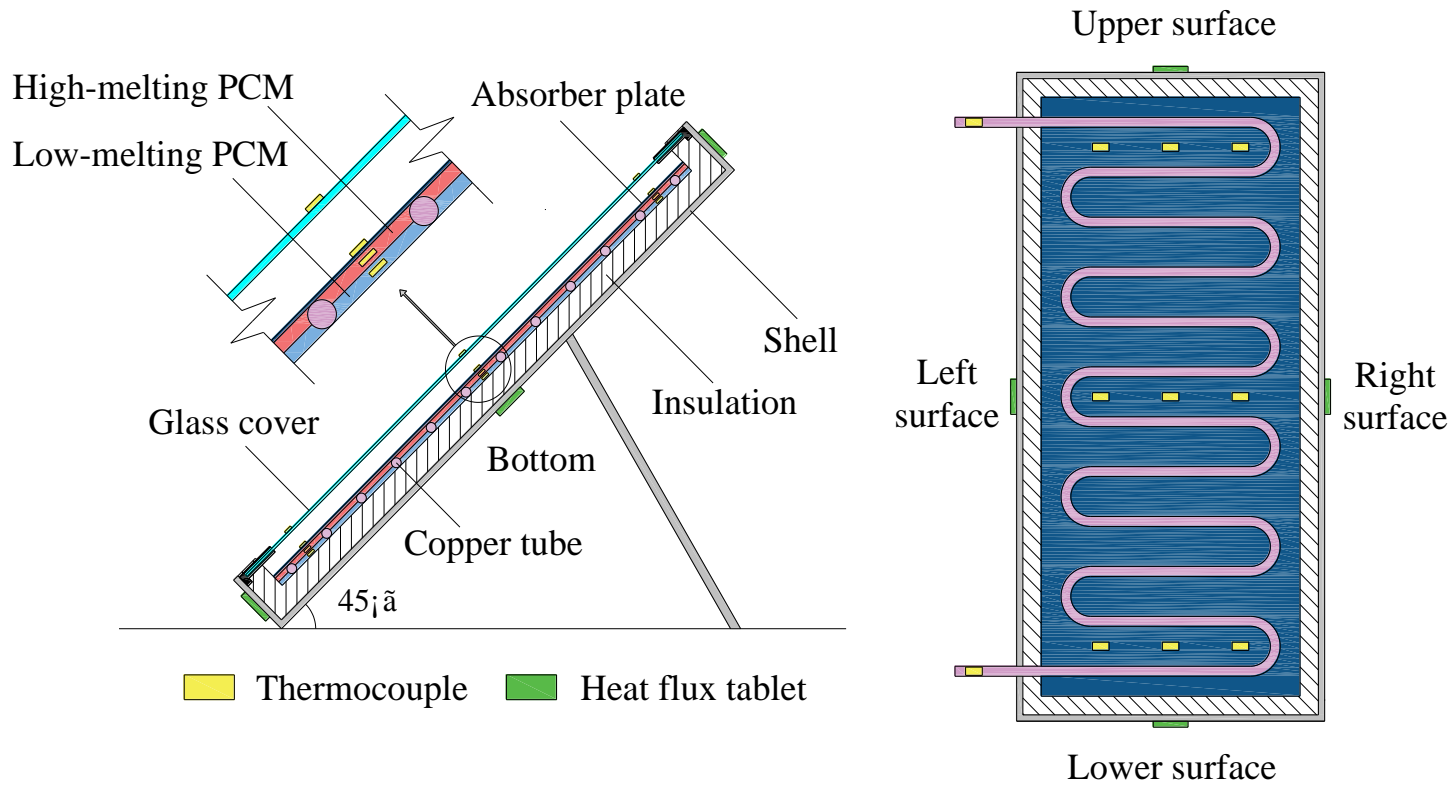


Fig. 1 Structure of the PCM collector and sensor locations

1  
2

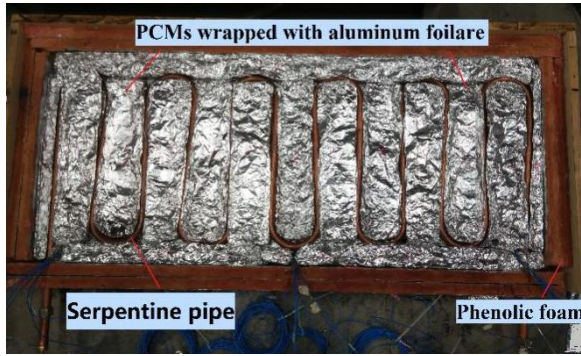


Fig. 2 Location of the PCMs in the collector

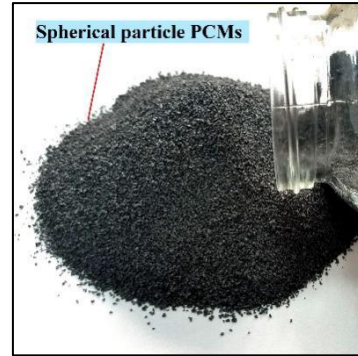


Fig. 3 Spherical particle PCMs

Table 1 Physical parameters of the two kinds of PCMs

Phase transition temperature (°C)	Latent heat (J/g)	Thermal Conductivity (W/(m·K))	Density (g/mL)	Specific heat capacity (J/(g·K))
15	190	3-5	0.87	2
70	210	3-5	0.97	2

Table 2 Design parameters of the collector

	Dimensions	1 m×0.5 m×0.12 m (Length × width × thickness)
	Spacing between the glass and the plate	30 mm
	Materials	Copper tube
	Arrangement	Serpentine pipeline
Pipeline	Pipe diameter	24 mm
	Pipe spacing	80 mm
	Materials	Low iron ultra-white glass
	Transmittance	92%
	Reflectivity	4%
Glass cover	Emissivity	10%
	Thickness	4 mm
	Thermal Conductivity	0.76 W/(m·K)
	Materials	Blue film
Absorber plate	Absorption rate	95%
	Thickness	0.4 mm
	Materials	Phenolic foam
Insulation	Thickness	40 mm

## 2.2 Experimental system setup

The indoor experimental system of PCM collector is established and as illustrated in Fig. 4. The system mainly includes a dual-PCM collector, an artificial solar simulator, a water tank, a pump, an electromagnetic flowmeter, an air-cooled condenser and several valves. A TRM-PD1 artificial solar simulator was used to provide solar radiation of which the adjustable extent is 600-1200 W/m<sup>2</sup>. The inlet water temperature was regulated by a temperature controller which was connected to a temperature sensor and an electric heater. An air-cooled condenser was used to cool the water heated by the collector. A pump was used to power the system. A magnetic flowmeter installed on the pipeline was used to measure and record the flow.



Fig. 4 Experimental system of a PCM collector

## 2.3 Operating conditions

High-temperature and low-temperature conditions were designed for the PCM collector. In high-temperature conditions, by using the temperature controller, the inlet water temperature was regulated to 30°C, 50°C, and 70°C. By adjusting the solar simulator, the solar radiation intensity

1 was set to approximately  $770 \text{ W/m}^2$  to make the outlet water temperature rising until it was stable  
2  
3 at the beginning of the operating conditions, then, the solar simulator was turned off, and under the  
4  
5 action of the condenser, the water temperature of the collector decreased until it was stable. Under  
6  
7 low-temperature conditions, the collector was laid in a closed artificial climate chamber where the  
8  
9 ambient temperature was set to  $9\text{-}10^\circ\text{C}$  to keep the temperature of the collector low until it was  
10  
11 stable. Then, the temperature control is stopped and the door of the climate chamber was opened  
12  
13 to keep the temperature rising. Under the same conditions, the collector without PCM was tested  
14  
15 and compared with the PCM collector. In addition, experiments on the positions of the two kinds  
16  
17 of PCMs were performed.  
18  
19  
20  
21  
22  
23  
24  
25

## 26 **2.4 Instrumentation**

27  
28 In the experiments, the temperatures of the glass cover, absorber plate, PCMs, inlet and outlet  
29  
30 water were recorded using a thermocouple with an accuracy of  $\pm 0.2\%$  (i.e.,  $\pm 1^\circ\text{C}$ ), and the  
31  
32 measuring range was  $-200^\circ\text{C}$  to  $200^\circ\text{C}$ . In addition, under high-temperature conditions, the heat  
33  
34 fluxes of the sidewall and bottom of the collector were measured using a heat flux meter with an  
35  
36 accuracy of  $\pm 2.0\%$ , and the heat flux meters were connected to a data acquisition instrument with  
37  
38 a measuring range of  $-1500$  to  $1500 \text{ W/m}^2$ . Under low-temperature conditions, the heat flux of the  
39  
40 glass cover was also measured. An anemometer with an accuracy of  $\pm 5\%$  (i.e.,  $\pm 0.05 \text{ m/s}$ ) was  
41  
42 installed at the height of the midpoint of the collector to measure the air velocity, and the  
43  
44 measuring range was  $0.05\text{--}30 \text{ m/s}$ . An automatic temperature recorder with an accuracy of  $\pm 5\%$   
45  
46 was placed near the collector to record the ambient temperature, and the measuring range was  $0$  to  
47  
48  $55^\circ\text{C}$ . A solar radiation meter with an accuracy of  $\pm 5\%$  was located in the same plane as the  
49  
50 glazing surface of the collector, and there was no shielding to the collector; thus the meter can  
51  
52  
53  
54  
55  
56  
57  
58  
59  
60  
61  
62  
63  
64  
65

1 accurately measure the solar radiation projected on the collector, and the measuring range is  
2  
3 0~2000 W/m<sup>2</sup>. The sampling period for all of the sensors was 30 s. The locations of the sensors  
4  
5  
6 are shown in Fig. 1. To reduce the effect of the environment on the inlet water temperature, the  
7  
8  
9 pipeline from the outlet of water tank to the inlet of collector was shortened as much as possible  
10  
11  
12 and the pipeline of the system was covered with insulation pipe and aluminum foil.

## 14 2.5 Efficiency calculation method and test procedure

17 For the flat plate collector, the instantaneous efficiency can be obtained by the calculation  
18  
19  
20 formula as follows [24]:

$$22 \eta = \frac{q_m c_p (T_o - T_i)}{A_a I} \quad (1)$$

23  
24  
25  
26  
27 where  $t_i$  is the inlet water temperature (°C),  $t_o$  is the outlet water temperature (°C),  $q_m$  is the  
28  
29  
30 mass flow rate of the water (kg/s),  $c_p$  is the specific heat capacity of the water (J/(kg·K)),  $A_a$   
31  
32 is the lighting area of the collector (m<sup>2</sup>), and  $I$  is the intensity of the solar radiation projected on  
33  
34  
35 the collector (W/m<sup>2</sup>).  
36

37  
38 During the indoor efficiency test experiment of the PCM collector in steady state, the  
39  
40  
41 collector was adjusted with respect to the solar simulator so that the solar radiation projected on  
42  
43  
44 the flat plate collector was vertically incident, and four evenly spaced inlet water temperature  
45  
46  
47 conditions (30°C, 40°C, 50°C and 60°C) were selected in the operating temperature range of the  
48  
49  
50 collector. The measurement process was divided into two phases: 12-minute preparation period  
51  
52  
53 and 12-minute steady-state measurement period. After a 12-minute preparation period, the system  
54  
55  
56 arrived in a steady state and the data record was started. The entire measurement process lasted for  
57  
58  
59  
60 12 minutes, and the average of the measured parameters within 12 minutes was taken for the  
61  
62  
63  
64  
65 efficiency calculation.

1 The instantaneous efficiency fitting curve of the collector is a linear fitting curve of the  
2 efficiency based on the lighting area and the inlet water temperature of the collector and should be  
3 fitted by at least four efficiency points. The formula is as follows:

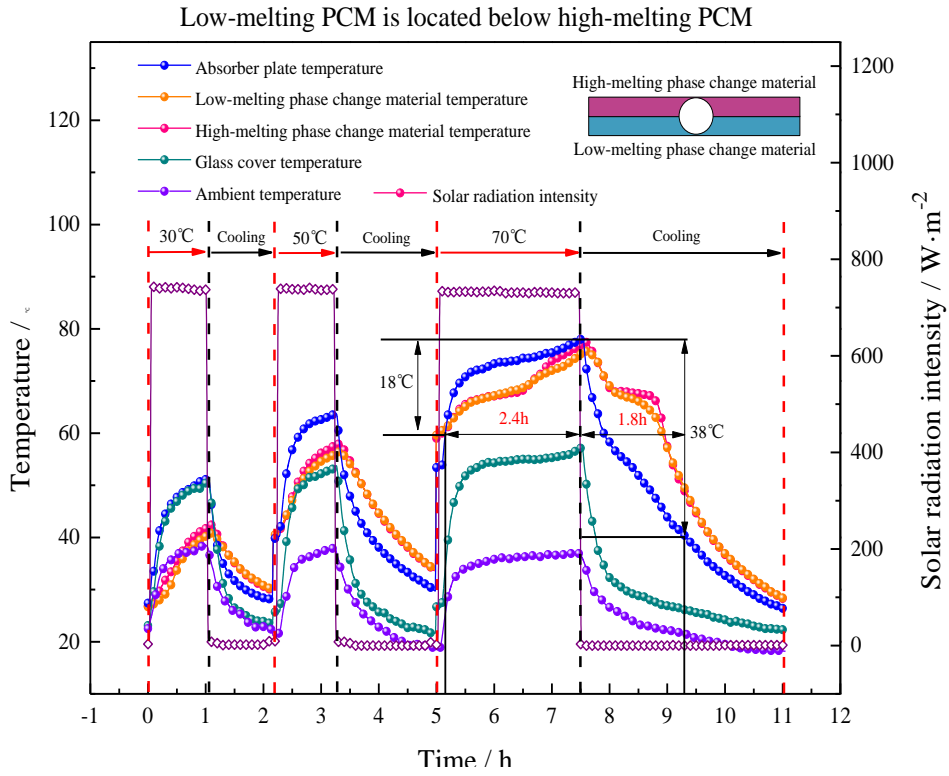
$$4 \quad \eta_a = \eta_{0,a} - UT_i^* \quad (2)$$

5 where  $T_i^* = (t_i - t_a)I$  is the normalized temperature difference based on the inlet temperature  
6  $((m^2 \cdot K)/W)$ ;  $t_a$  is the ambient temperature ( $^{\circ}C$ );  $\eta_{0,a}$  is the instantaneous efficiency intercept  
7 based on the lighting area and inlet temperature of the collector, which mainly depends on the  
8 optical characteristics of the glass cover, the absorber and the number of cover layers, and the  
9 value of this variable indicates the highest efficiency that the collector can theoretically achieve;  
10 the slope  $U$  is the heat loss coefficient of collector with respect to  $T_i^*$ , which mainly depends  
11 on the configuration and thermal insulation performance of the collector.

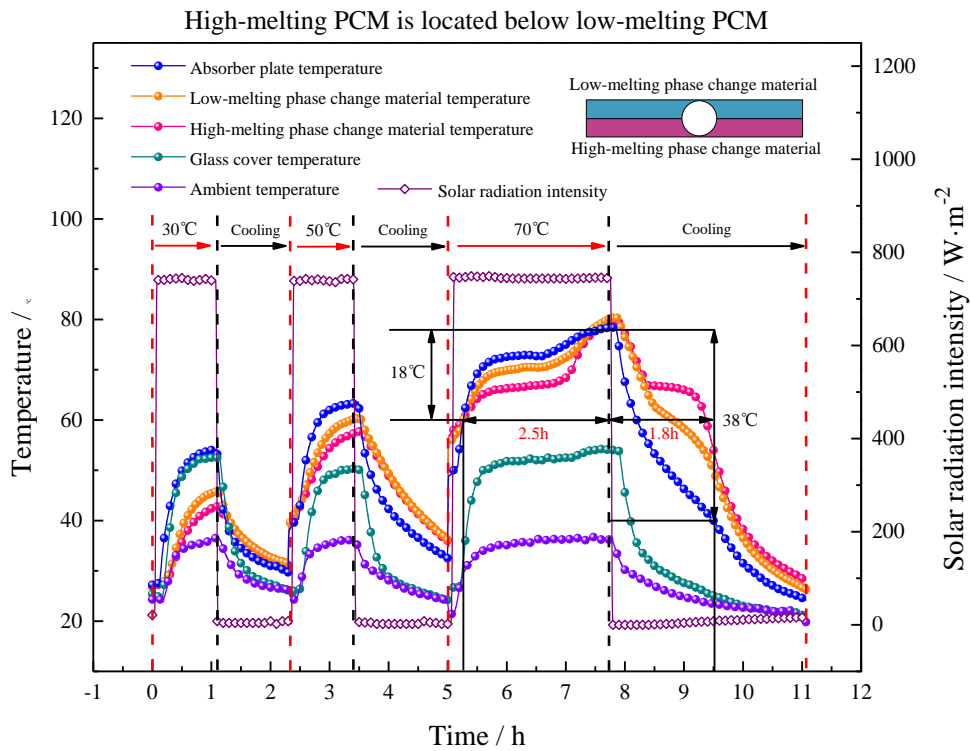
### 13 **3. Experimental results**

#### 14 **3.1 Temperature and heat flux under high-temperature conditions**

15 The temperatures of measuring points in the PCM collector and conventional collector for  
16 various water temperatures in high-temperature conditions are shown in Fig. 5, and the heat fluxes  
17 of sidewall and bottom are shown in Fig. 6.

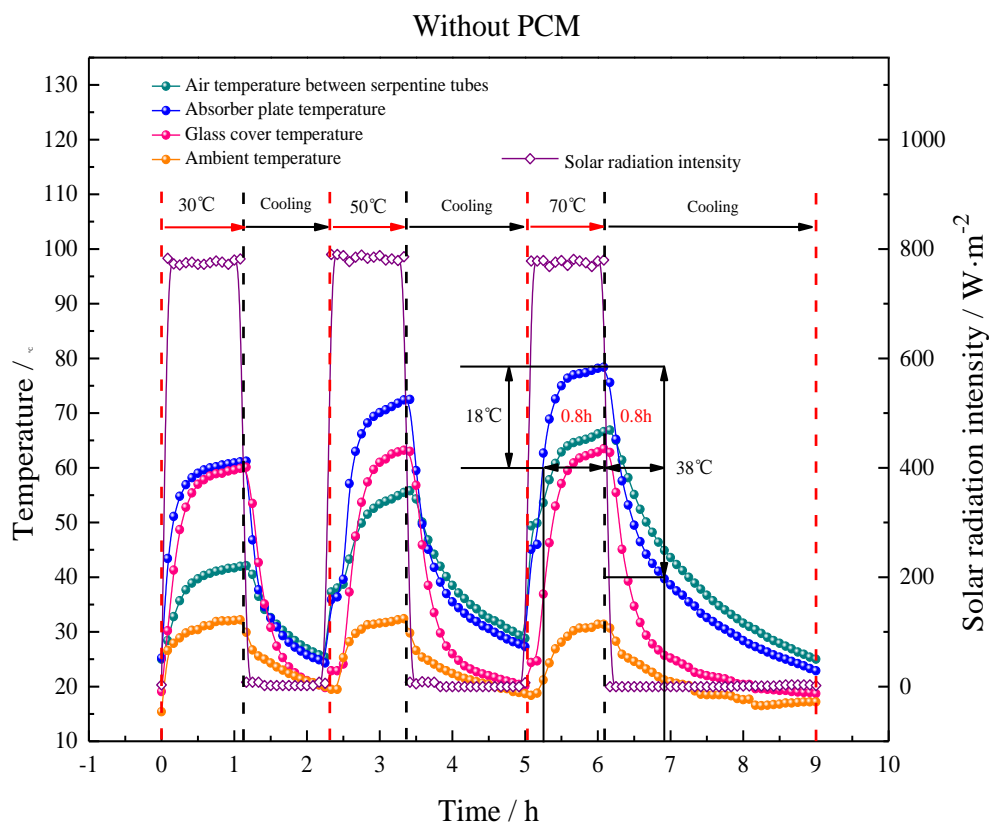


(a) Low-melting PCM underneath the high-melting PCM



(b) High-melting PCM underneath the low-melting PCM

1  
2  
3  
4  
5  
6  
7  
8  
9  
10  
11  
12  
13  
14  
15  
16  
17  
18  
19  
20  
21  
22  
23  
24  
25  
26  
27  
28  
29  
30  
31  
32  
33  
34  
35  
36  
37  
38  
39  
40  
41  
42  
43  
44  
45  
46  
47  
48  
49  
50  
51  
52  
53  
54  
55  
56  
57  
58  
59  
60  
61  
62  
63  
64  
65



(c) Without PCM

Fig.5 Temperatures of the measuring points in the collector under high-temperature conditions

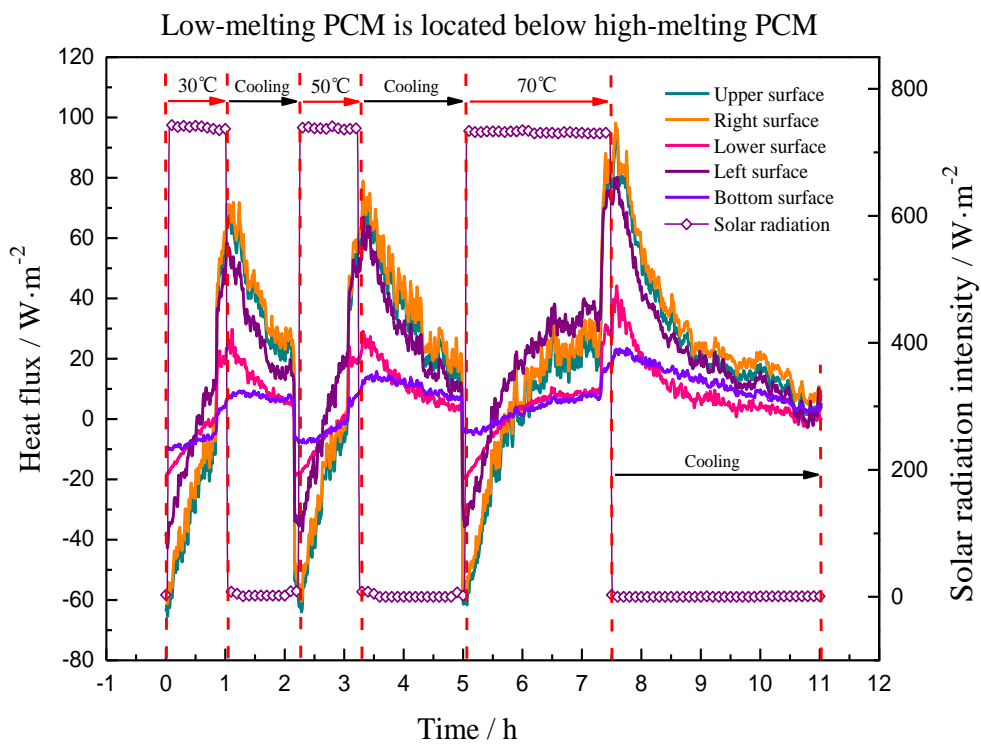
It can be seen from Fig. 5 that in the case of 30°C and 50°C water temperature conditions, after solar simulator was switched on, the temperature of absorber, glass cover and PCMs in all cases ((a), (b) and (c)) increased rapidly within approximately 1 h and then tended to stabilize. After solar simulator was switched off, the temperature dropped rapidly. For the collector without PCM (case (c)), the temperature change under 70°C water temperature condition was similar to that under 30°C and 50°C water temperature conditions. However, for the collector with PCM (case (a) and (b)) and subjected to a 70°C water temperature condition, after the solar radiation was turned on, the temperature of the PCMs and the absorber plate increased rapidly within 0.5 h, then the temperature of the high-melting PCM reached the melting point and the temperature

1 curves of absorber plate and low-melting PCM tended to flatten due to the melting of the  
2 high-melting PCM. After all the high-melting PCM was melted, the temperature of the absorber  
3 and PCMs increased rapidly again and tended to stabilize. After the solar simulator was turned off,  
4 the temperature curves of the absorber and PCM dropped rapidly within 0.5 h; then the  
5 high-melting PCM began to solidify and release heat because the temperature reached the freezing  
6 point, the temperature tended to stabilize. Meanwhile, the temperature decrease rate of the  
7 absorber and low-melting PCM was lowered. After all the high-melting PCM was solidified, the  
8 temperature curves of the absorber plate and the PCMs began to drop rapidly again.

9 Moreover, as shown in Fig. 5, it took 2.4 h, 2.5h and 0.8 h for the absorber plate temperature  
10 to increase from 60 °C to 78 °C for the case (a), (b) and (c), respectively, and it took 1.8 h, 1.8h  
11 and 0.8 h for the absorber plate temperature to decrease from 78 °C to 40 °C, respectively.  
12 According to the time comparison, it can be found that the time taken for the heating and cooling  
13 process of the PCM collector was significantly longer than that of the conventional collector,  
14 which mainly occurred because the high-melting PCM absorbed heat during melting and released  
15 heat during solidification. The time taken for the heating process of the case (b) was slightly  
16 longer than that of the case (a) because the thermal resistance between the absorber plate and the  
17 high-melting PCM was larger when the high-melting PCM is located below the low-melting PCM.  
18 However, the time difference between the case (a) and (b) was small due to the high thermal  
19 conductivity of the PCMs.

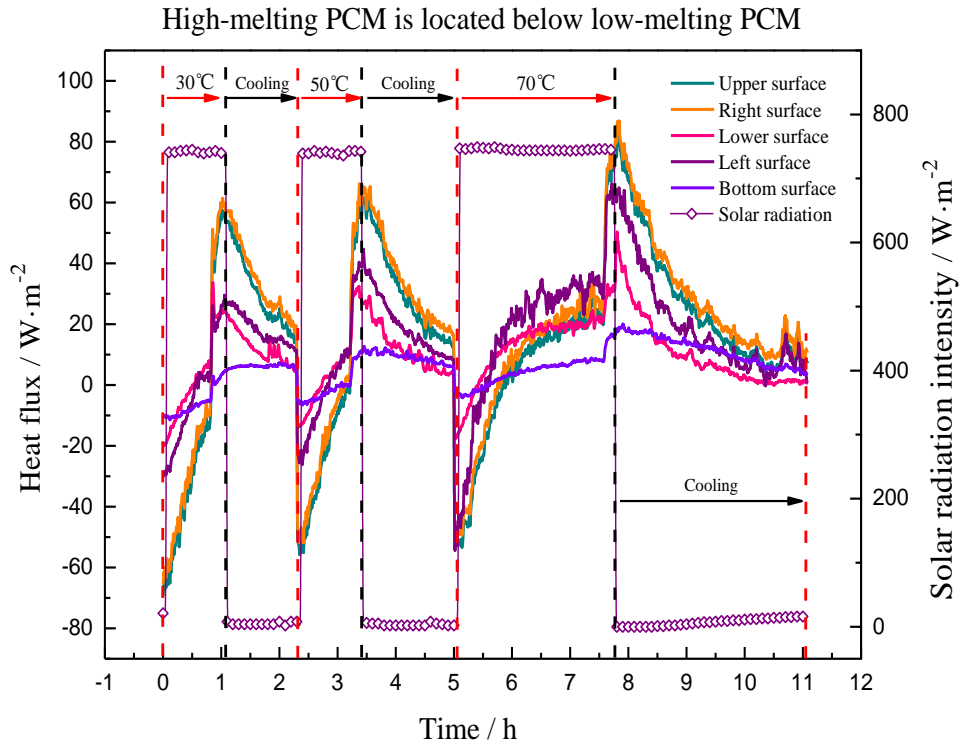
20 It can be seen from the above-mentioned analytical result that the high-melting PCM can  
21 store heat when the high water temperature of the pipe leads to the high-melting PCM melting,  
22 and the time when the temperature reaches the maximum is delayed, thus decrease the temperature

1 rising rate of the collector and relieving overheating. When the water temperature of the collector  
 2 decreases with the reduction of solar radiation, the accumulation of heat in the high-melting PCM  
 3 can be used to decrease the temperature drop rate of the collector, thereby improving the thermal  
 4 performance of the collector in low or no solar radiation conditions. In addition, when the  
 5 high-melting PCM is located below the low-melting PCM, the delay effect of the high-melting  
 6 PCM on the time when the temperature reaches the maximum is more obvious.

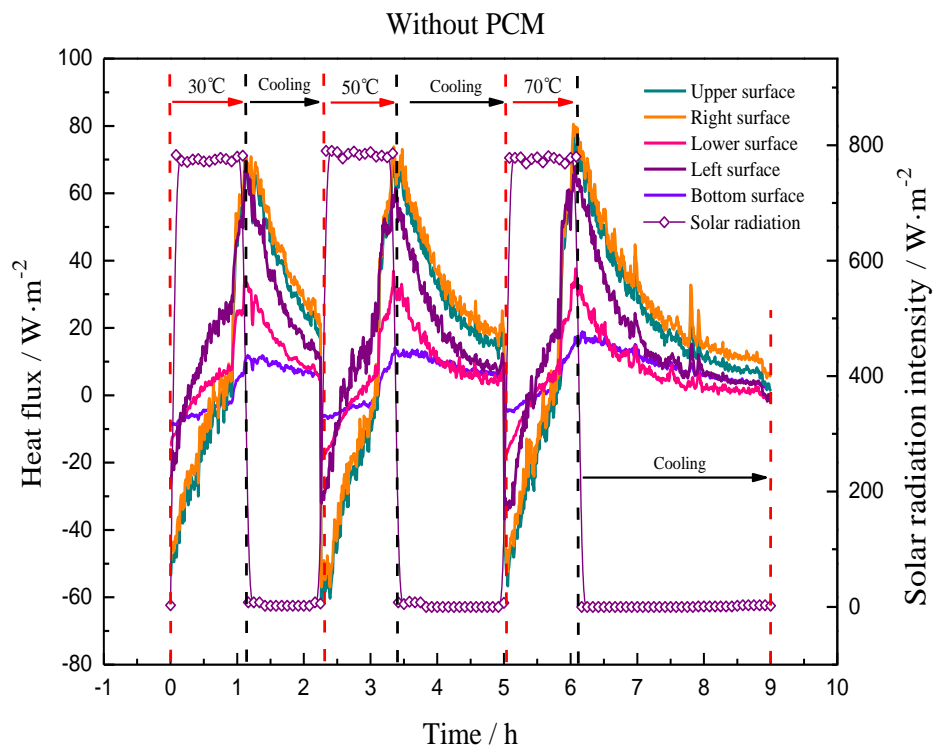


Heat flux: The heat flux transferred from the collector to the environment is positive.

(a) Low-melting PCM is located below the high-melting PCM



(b) High-melting PCM is located below the low-melting PCM



(c) Without PCM

Fig. 6 Heat flow variations in the PCM collector in high-temperature conditions

1  
2  
3  
4  
5  
6  
7  
8  
9  
10  
11  
12  
13  
14  
15  
16  
17  
18  
19  
20  
21  
22  
23  
24  
25  
26  
27  
28  
29  
30  
31  
32  
33  
34  
35  
36  
37  
38  
39  
40  
41  
42  
43  
44  
45  
46  
47  
48  
49  
50  
51  
52  
53  
54  
55  
56  
57  
58  
59  
60  
61  
62  
63  
64  
65

1  
2 As shown in Fig. 6, under the water temperature conditions of 30 °C and 50 °C, after solar  
3 simulator was switched on, as the temperature of collector increased, the heat fluxes transferred  
4 from the collector to the environment changed from negative to positive and increase until the  
5 solar radiation was turned off. Meanwhile, the variation trend of the heat fluxes of the  
6 conventional collector was similar to that of the PCM collector. Under the water temperature  
7 condition of 70 °C, the heat fluxes of the sidewall and bottom of the PCM collector increased  
8 slowly in the melting process of the high-melting PCM. During the solidification process, as the  
9 temperature of the collector gradually decreased and was close to the environment temperature,  
10 the heat fluxes of the collector approached zero, and the trend of heat fluxes dropping slowly was  
11 not obvious; however, compared with the conventional collector, the time had been prolonged.  
12 The above analysis shows that when the high water temperature of pipe leads to the high-melting  
13 PCM melting, the high-melting PCM can slow the heat absorption of collector, and when water  
14 temperature drops, the accumulation of heat in the PCM can be effectively utilized to slow the  
15 heat dissipation process of the collector.

### 16 17 **3.2 Temperature and heat flux under low-temperature conditions**

18 The temperatures of the measuring points in the PCM collector and conventional collector  
19 under low-temperature conditions are shown in Fig. 7, and the heat fluxes of the sidewall, bottom  
20 and glass cover are shown in Fig. 8.

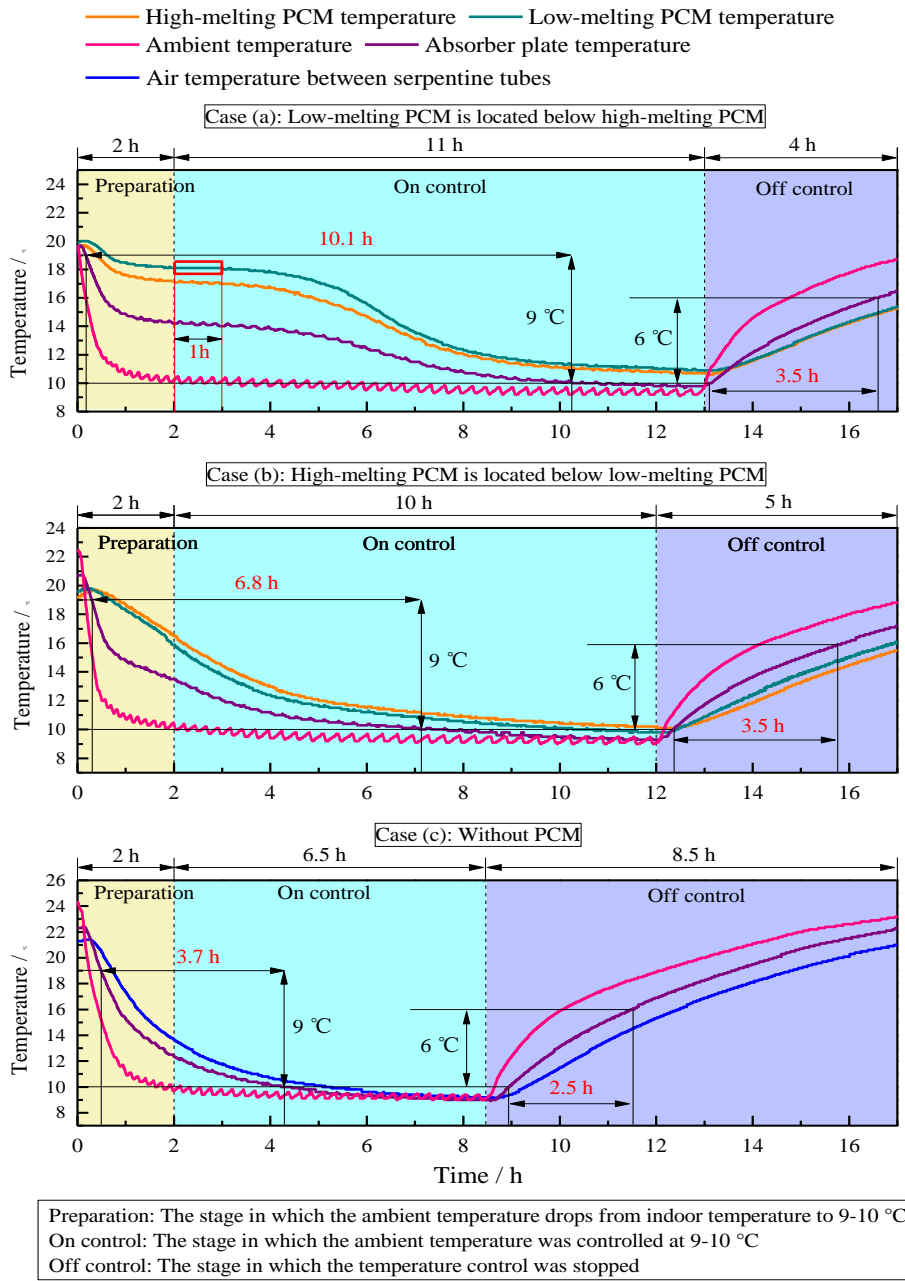
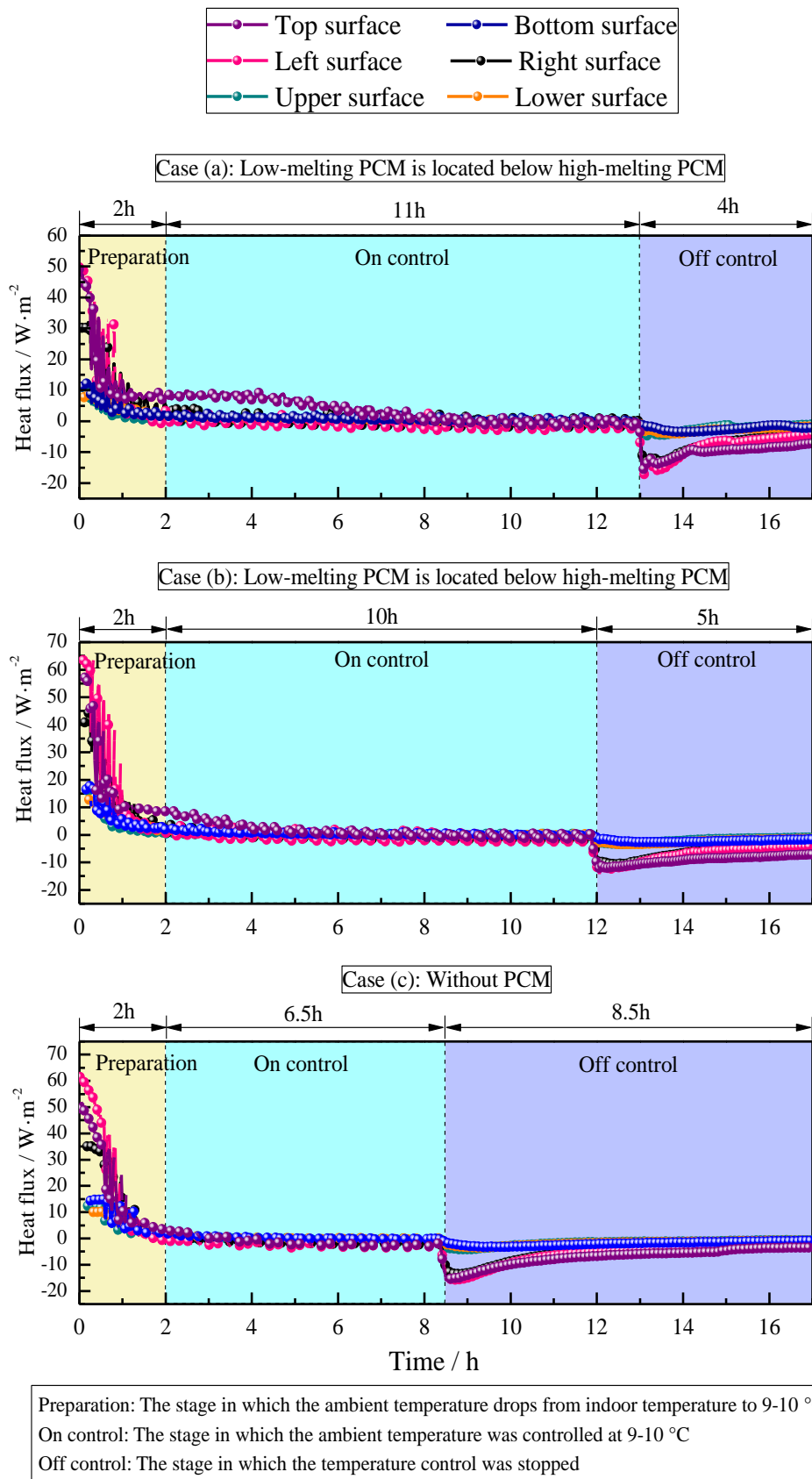


Fig. 7 Temperature variations in the PCM collector under low-temperature conditions

As shown in Fig. 7, compared with the collector without PCM, when the low-melting PCM was located below high-melting PCM, the temperature of PCMs and absorber was lowered rapidly with the decrease of the ambient temperature at the beginning. After that, the temperature curves dropped slowly because the temperature of the low-melting PCM decreased to the freezing point

1 and the low-melting PCM began to solidify and release heat. At the same time, there was an  
2 obvious one-hour constant temperature interval for the low-melting PCM, which indicates that the  
3 low-melting PCM can obviously slow the temperature decrease rate of absorber and relieve the  
4 freezing problem of flat plate collector in the low-temperature environment. There was a tendency  
5 to drop slowly for the temperature curve of absorber when the high-melting PCM was located  
6 below low-melting PCM. However, the constant temperature interval did not exist in the  
7 temperature curve of the low-melting PCM, it can be mainly interpreted as the low-melting PCM  
8 located above the high-melting PCM was greatly affected by the environment temperature,  
9 resulting in a fast phase change. On the contrary, compared with the conventional collector, the  
10 temperature of the PCM collector decreased more slowly.

11 As shown in Fig. 7, it took 10.1 h, 6.8 h and 3.7 h for the absorber plate temperature to  
12 decrease from 19 °C to 10 °C for the case (a), (b) and (c), respectively, this indicates that the  
13 time taken for the cooling process can be prolonged by the solidification exotherm of the  
14 low-melting PCM. When the temperature control was stopped, as the environment temperature  
15 increased, the temperature of the collector gradually increased. As shown in Fig. 7, it took 3.5 h,  
16 3.5 h and 2.5 h for the absorber plate temperature to increase from 10 °C to 16 °C for the case  
17 (a), (b) and (c), respectively, which shows that the time taken for the temperature rising process of  
18 the PCM collector is longer because of the heat absorption of low-melting PCM during the  
19 melting process.



1  
2 Fig. 8 Heat flow variations in the PCM collector under high-temperature conditions

1  
2  
3  
4 2 It can be seen from Fig. 8 that the heat fluxes of the sidewall and the bottom of the collector  
5  
6 3 decreased rapidly with decreasing air temperature and quickly approached zero for the case (a), (b)  
7  
8 4 and (c), which shows that the temperatures of the sidewall and the bottom are close to the  
9  
10 5 environment temperature, and the heat exchange between them approaches zero at this time.  
11  
12 6 Furthermore, the heat flux of the glass cover tended to stabilize within two hours after the second  
13  
14 7 hour when the low-melting PCM was located below the high-melting PCM (case (a)). Even  
15  
16 8 though there was an increasing trend in the middle of the process, indicating that the temperature  
17  
18 9 of the air layer in the PCM collector was higher than the environment temperature due to the heat  
19  
20 10 release of the low-melting PCM during solidification. All of these properties are beneficial to the  
21  
22 11 antifreeze performance of the collector. When the high-melting PCM was located below the  
23  
24 12 low-melting PCM (case (b)), the trend of the heat flux decreasing slowly was less obvious, but the  
25  
26 13 time when the heat flux of the glass cover dropped to zero was still delayed. When the door of the  
27  
28 14 climate chamber was opened and the ambient temperature increased rapidly, the heat fluxes  
29  
30 15 quickly dropped from zero to a negative value and then slowly increased and approached zero, and  
31  
32 16 the duration of this process of the PCM collector was substantially longer than that of the  
33  
34 17 conventional collector. According to the comprehensive analysis of temperature and heat flow, the  
35  
36 18 following conclusion can be drawn: placing the low-melting PCM below the high-melting PCM  
37  
38 19 provided the greatest frost resistance to the collector.  
39  
40  
41  
42  
43  
44  
45  
46  
47  
48  
49  
50  
51  
52  
53  
54  
55  
56  
57  
58  
59  
60  
61  
62  
63  
64  
65

## 21 **4. Discussion and analysis**

### 22 **4.1 Time analysis**

1 Compared with the conventional collector, in the 70 °C water temperature condition, the  
2  
3 time taken for the temperature of the absorber plate to increase from 60 °C to 78 °C could be  
4  
5 prolonged by 1.6 h and 1.7 h for the case (a) and case (b), respectively, which could reduce  
6  
7 overheating problems of the collector. The time taken for the temperature of the absorber plate to  
8  
9 decrease from 78 °C to 40 °C could be prolonged by 1 h for the case (a) and case (b), which  
10  
11 indicates that the heat stored in the high-melting PCM can be effectively used to enhance the  
12  
13 thermal performance during the cooling process. According to the time comparison, the prolonged  
14  
15 time was longer when the high-melting PCM was located below the low-melting PCM, but the  
16  
17 difference was not significant.  
18  
19  
20  
21  
22  
23  
24

25 Under a 9-10°C low-temperature environment, the time taken for the temperature of the  
26  
27 absorber plate to decrease from 19 °C to 10 °C could be prolonged by 6.4 h and 3.1 h for the  
28  
29 case (a) and (b), respectively, which can reduce freezing problems of the collector. According to  
30  
31 the time comparison, when the low-melting PCM was located below the high-melting PCM, the  
32  
33 antifreeze effect of the PCM on the collector was more substantial.  
34  
35  
36  
37  
38  
39  
40  
41

## 42 **4.2 Efficiency analysis**

43  
44 According to the efficiency calculation method, the efficiencies of the collector were  
45  
46 calculated in the four inlet water temperature conditions (30°C, 40°C, 50°C and 60°C), and the  
47  
48 efficiency curves of the PCM collector and conventional collector were obtained and compared, as  
49  
50 shown in Fig. 9. The efficiency of the collector obtained by the experiment was low, mainly  
51  
52 because the collector was assembled by the experimenter and did not have good sealing  
53  
54 performance; this low sealing performed caused large heat loss, but the effect of PCMs on the  
55  
56  
57  
58  
59  
60  
61  
62  
63  
64  
65

1 efficiency of the collector can still be reflected by comparing the relative values of different  
 2 efficiencies.

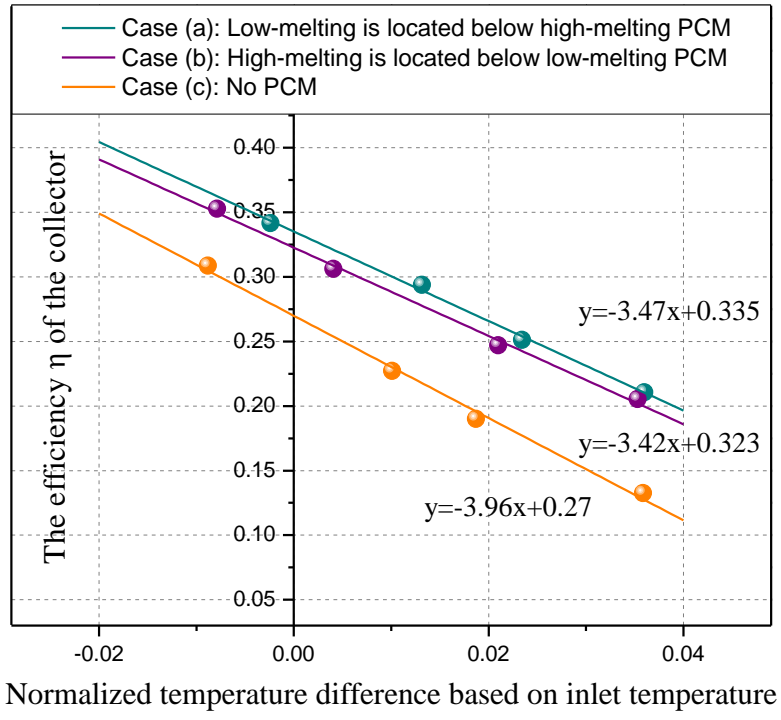


Fig. 9 Efficiencies of the PCM collector and conventional collector

7 Fig. 9 compared the efficiency of traditional collector with the PCM collectors. The  
 8 efficiency of the PCM collector in case (a) and case (b) was increased by 24.1% and 19.6%,  
 9 respectively. The increased efficiency mainly occurs because the air below the absorber plate in  
 10 the conventional collector was filled with PCMs, and the thermal resistance between the absorber  
 11 plate and the pipe was smaller due to the high thermal conductivity of the PCMs.

13 **5. Conclusions**

14 In this study, a new dual-PCM collector was proposed that can relieving the freezing and

1 overheating problems of a flat plate collector, and experiments were conducted to study the heat  
2 transfer process and thermal performance of the dual-PCM collector; the efficiency of the  
3 dual-PCM collector was then compared to that of a traditional collector. The research obtains the  
4 following detailed conclusions:

5 (1) In the case of high water temperature, the high-melting PCM in the PCM collector can  
6 decrease the temperature rising rate of the collector by melting and absorbing heat. The time  
7 taken for the temperature of the absorber plate to rise from 60 °C to 78 °C can be  
8 prolonged by 1.6 h and 1.7 h when the low-melting PCM placed below the high-melting  
9 PCM and in the opposite condition, which can relieve overheating problems of the collector.

10 When the water temperature is lowered, the excess heat stored by the high-melting PCM can  
11 be effectively utilized to enhance the thermal performance of the collector. The heat fluxes of  
12 sidewall and bottom also increase slowly due to the melting of the high-melting PCM in the  
13 heating process.

14 (2) In the case of low temperature, the low-melting PCM of the PCM collector can solidify and  
15 release heat to substantially slow the cooling of the collector. When the low-melting PCM  
16 placed below the high-melting PCM and in the opposite condition, the time taken for the  
17 temperature of the absorber plate to decrease from 19 °C to 10 °C could be prolonged by  
18 6.4 h and 3.1 h, respectively, thereby relieving the freezing problems of the collector. During  
19 the exothermic solidification of the low-melting PCM, the temperature of the air layer is  
20 higher than the ambient temperature, which is beneficial to the antifreeze of the collector.

21 (3) Compared with a conventional collector, the efficiency of the PCM collector when placing  
22 the low-melting PCM below the high-melting PCM and in the opposite condition is increased

1 by 24.1% and 19.6%, respectively.

2

### 3 **References**

- 4 [1] Harrison S , Cruickshank C A. A review of strategies for the control of high temperature  
5 stagnation in solar collectors and systems. *Energy Procedia*, 2012, 30:793-804.
- 6 [2] Wilcox B A, Barnaby C S. Freeze protection for flat-plate collectors using heating. *Sol.*  
7 *Energy*, 1977, 19(6):745-746.
- 8 [3] Crofoot L, Harrison S. Performance Evaluation of a Liquid Desiccant Solar Air Conditioning  
9 System. *Energy Procedia*, 2012, 30(30):542-550.
- 10 [4] Kessentini H, Castro J, Capdevila R, et al. Development of flat plate collector with plastic  
11 transparent insulation and low-cost overheating protection system. *Appl. Energy*, 2014,  
12 133:206-223.
- 13 [5] Hussain S, Harrison S J. Experimental and numerical investigations of passive air cooling of  
14 a residential flat-plate solar collector under stagnation conditions. *Sol. Energy*, 2015,  
15 122:1023-1036.
- 16 [6] Hussain S, Harrison S J . Evaluation of thermal characteristics of a flat plate Solar Collector  
17 with a back mounted air channel. *Appl. Therm. Eng*, 2017, 123:940-952.
- 18 [7] Gladen A C, Davidson J H, Mantell S C. Selection of thermotropic materials for overheating  
19 protection of polymer absorbers. *Sol. Energy*, 2014, 104:42-51.
- 20 [8] Resch K, Wallner G M. Thermotropic layers for flat-plate collectors—A review of various  
21 concepts for overheating protection with polymeric materials. *Solar Energy Materials &*  
22 *Solar Cells*, 2009, 93(1):119-128.

- 1 [9] Wallner G M, Resch K, Hausner R. Property and performance requirements for thermotropic  
2 layers to prevent overheating in an all polymeric flat-plate collector. *Solar Energy Materials*  
3 and *Solar Cells*, 2008, 92(6):614-620.
- 4 [10] Koenigshofer D R. Freeze protection for solar collectors. *Sunworld*, 1977.
- 5 [11] Yikang W, Wenhua X, Jun Y, et al. The antifreeze mechanism of flat plate-type solar  
6 collector and material characteristics of absorber plate// *The New Solar Energy Technology*  
7 in the 21st Century: the Monograph of Academic Annual Conference. Shanghai: Shanghai  
8 Jiaotong University Press, 2003: 407-410.
- 9 [12] Jiang X, Zhen T, Lu J, et al. Theoretical and experimental studies on sequential freezing solar  
10 water heater. *Sol. Energy*, 1994, 53(2):139-146.
- 11 [13] Ozsoy A, Demirer S, Adam N M. An Experimental Study on Double-Glazed Flat Plate Solar  
12 Water Heating System in Turkey. *Applied Mechanics and Materials*, 2014, 564:204-209.
- 13 [14] Reddy K S, Kaushika N D. Comparative study of transparent insulation materials cover  
14 systems for integrated-collector-storage solar water heaters. *Solar Energy Materials and Solar*  
15 *Cells*, 1999, 58(4):431-446.
- 16 [15] Zhou F, Jie J, Jingyong C, et al. Experimental and numerical study of the freezing process of  
17 flat-plate solar collector. *Appl. Therm. Eng*, 2017, 118: 773-784.
- 18 [16] Wenjia Su, Ran Z, Zhiqiang Z, et al. Flat Plate solar Collector/Storage System. *Acta Energiæ*  
19 *Solaris Sinica*, 2008, 29(4): 449-453.
- 20 [17] A.E.Kabeel, A.Khalil, S.M.Shalaby, et al. Experimental investigation of thermal performance  
21 of flat and v-corrugated plate solar air heaters with and without PCM as thermal energy  
22 storage. *Energy Conversion and Management*, 2016, 113: 264-272.

- 1 [18] CHEN Z, GU M, Peng D. Heat transfer performance analysis of a solar flat-plate collector  
2 with an integrated metal foam porous structure filled with paraffin. *Appl. Therm. Eng*, 2010,  
3 30(14): 1967-1973.
- 4 [19] Jing Z, Zhiping W, Kezhen W, et al. The design and research of anti-freezing solar flat plate  
5 collector with phase change energy storage layer. *Journal of Central South University*  
6 (Science and Technology), 2016, 47(10): 3575-3581.
- 7 [20] Khalifa A J N, Suffer K H, Mahmoud M S. A storage domestic solar hot water system with a  
8 back layer of phase change material. *Experimental Thermal and Fluid Science*, 2013, 44:  
9 174-181.
- 10 [21] Mettawee E B S, Assassa G M R. Experimental study of a compact PCM solar collector.  
11 *Energy*, 2006, 31(14): 2958-2968.
- 12 [22] Mettawee E B S, Assassa G M R. Thermal conductivity enhancement in a latent heat storage  
13 system. *Sol. Energy*, 2007, 81(7): 839-845.
- 14 [23] Varol Y, Koca A, Oztop H F, et al. Forecasting of thermal energy storage performance of  
15 Phase Change Material in a solar collector using soft computing techniques. *Expert Systems*  
16 with Applications, 2010, 37(4): 2724-2732.
- 17 [24] General Administration of Quality Supervision, Inspection and Quarantine of the People's  
18 Republic of China. "GB/T 4271-2007" Test methods for the thermal performance of solar  
19 collectors. Beijing: China Standard Press, 2007.
- 20 [25] Zhou, F., Ji, J., Yuan, W., Zhao, X. & Huang, S. Study on the PCM flat-plate solar collector  
21 system with antifreeze characteristics. *International Journal of Heat and Mass Transfer* 129,  
22 357-366, doi:<https://doi.org/10.1016/j.ijheatmasstransfer.2018.09.114> (2019).

1 [26] Charvát, P., Klimeš, L., Pech, O. & Hejčík, J. Solar air collector with the solar absorber plate  
 2 containing a PCM – Environmental chamber experiments and computer simulations. Renewable  
 3 Energy 143, 731-740, doi:<https://doi.org/10.1016/j.renene.2019.05.049> (2019).  
 4

<b>Nomenclature</b>	
$\eta$	Instantaneous efficiency
$t_i$	Inlet water temperature (°C)
$t_o$	Outlet water temperature (°C)
$q_m$	Mass flow of the water (kg/s)
$c_p$	Specific heat capacity of the water (J/(kg·K))
$A_a$	Lighting area of the collector (m <sup>2</sup> )
$I$	The intensity of the solar radiation projected on the collector (W/m <sup>2</sup> )
$T_i^*$	Normalized temperature difference based on the inlet temperature ((m <sup>2</sup> ·K)/W)
$t_a$	Ambient temperature (°C)
$\eta_{0,a}$	Instantaneous efficiency intercept based on the lighting area and inlet temperature of the collector
$U$	Heat loss coefficient of the collector with reference to $T_i^*$
<b>Subscripts</b>	
$i$	Inlet
$o$	Outlet
$a$	Ambient